National Bureau of Standards
Library, E-01 Admin. Bldg.
MAY 15 1970
cop. 2.

NBS TECHNICAL NOTE 527

ITED STATES
RTMENT OF
MMERCE
LICATION

Methods of Measurement for Semiconductor Materials, Process Control, and Devices

Quarterly Report

October 1 to December 31, 1969

U.S.
ARTMENT
OF
MMERCE
National
Bureau
of
Standards

NATIONAL BUREAU OF STANDARDS

The National Bureau of Standards [1] was established by an act of Congress March 3, 1901. Today, in addition to serving as the Nation's central measurement laboratory, the Bureau is a principal focal point in the Federal Government for assuring maximum application of the physical and engineering sciences to the advancement of technology in industry and commerce. To this end the Bureau conducts research and provides central national services in four broad program areas. These are: (1) basic measurements and standards, (2) materials measurements and standards, (3) technological measurements and standards, and (4) transfer of technology.

The Bureau comprises the Institute for Basic Standards, the Institute for Materials Researeh, the Institute for Applied Technology, the Center for Radiation Research, the Center for Computer Sciences and Technology, and the Office for Information Programs.

THE INSTITUTE FOR BASIC STANDARDS provides the central basis within the United States of a complete and consistent system of physical measurement; coordinates that system with measurement systems of other nations; and furnishes essential services leading to accurate and uniform physical measurements throughout the Nation's scientific community, industry, and commerce. The Institute consists of an Office of Measurement Services and the following technical divisions:

Applied Mathematics—Electricity—Metrology—Mechanics—Heat—Atomic and Molecular Physics—Radio Physics [2]—Radio Engineering [2]—Time and Frequency [2]—Astrophysics [2]—Cryogenics.[2]

THE INSTITUTE FOR MATERIALS RESEARCH conducts materials research leading to improved methods of measurement standards, and data on the properties of well-characterized materials needed by industry, commerce, educational institutions, and Government; develops, produces, and distributes standard reference materials; relates the physical and chemical properties of materials to their behavior and their interaction with their environments; and provides advisory and research services to other Government agencies. The Institute consists of an Office of Standard Reference Materials and the following divisions:

Analytical Chemistry—Polymers—Metallurgy—Inorganic Materials—Physical Chemistry.

THE INSTITUTE FOR APPLIED TECHNOLOGY provides technical services to promote the use of available technology and to facilitate technological innovation in industry and Government; cooperates with public and private organizations in the development of technological standards, and test methodologies; and provides advisory and research services for Federal, state, and local government agencies. The Institute consists of the following technical divisions and offices:

Engineering Standards—Weights and Measures — Invention and Innovation — Vehicle Systems Research—Product Evaluation—Building Research—Instrument Shops—Measurement Engineering—Electronic Technology—Technical Analysis.

THE CENTER FOR RADIATION RESEARCH engages in research, measurement, and application of radiation to the solution of Bureau mission problems and the problems of other agencies and institutions. The Center consists of the following divisions:

Reactor Radiation—Linac Radiation—Nuclear Radiation—Applied Radiation.

THE CENTER FOR COMPUTER SCIENCES AND TECHNOLOGY conducts research and provides technical services designed to aid Government agencies in the selection, acquisition, and effective use of automatic data processing equipment; and serves as the principal focus for the development of Federal standards for automatic data processing equipment, techniques, and computer languages. The Center consists of the following offices and divisions:

Information Processing Standards—Computer Information — Computer Services — Systems Development—Information Processing Technology.

THE OFFICE FOR INFORMATION PROGRAMS promotes optimum dissemination and accessibility of scientific information generated within NBS and other agencies of the Federal Government; promotes the development of the National Standard Reference Data System and a system of information analysis centers dealing with the broader aspects of the National Measurement System, and provides appropriate services to ensure that the NBS staff has optimum accessibility to the scientific information of the world. The Office consists of the following organizational units:

Office of Standard Reference Data—Clearinghouse for Federal Scientific and Technical Information [3]—Office of Technical Information and Publications—Library—Office of Public Information—Office of International Relations.

---

[1] Headquarters and Laboratories at Gaithersburg, Maryland, unless otherwise noted; mailing address Washington, D.C. 20234.
[2] Located at Boulder, Colorado 80302.
[3] Located at 5285 Port Royal Road, Springfield, Virginia 22151.

UNITED STATES DEPARTMENT OF COMMERCE
Maurice H. Stans, Secretary
NATIONAL BUREAU OF STANDARDS • Lewis M. Branscomb, Director

NBS TECHNICAL NOTE 527

ISSUED MAY 1970

Nat. Bur. Stand. (U.S.), Tech. Note 527, 60 pages (May 1970)
CODEN: NBTNA

Methods of Measurement for Semiconductor Materials, Process Control, and Devices

Quarterly Report
October 1 to December 31, 1969

Edited by W. Murray Bullis

Electronic Technology Division
Institute for Applied Technology
National Bureau of Standards
Washington, D.C. 20234

Jointly Supported by the National Bureau of Standards, the Defense Atomic Support Agency, the U.S. Navy Strategic Systems Project Office, and the National Aeronautics and Space Administration

NBS Technical Notes are designed to supplement the Bureau's regular publications program. They provide a means for making available scientific data that are of transient or limited interest. Technical Notes may be listed or referred to in the open literature.

For sale by the Superintendent of Documents, U.S. Government Printing Office, Washington, D.C., 20402.
(Order by SD Catalog No. C13.46:527). Price 60 cents.

CONTENTS

PAGE

1. Introduction and Highlights 1

2. Methods of Measurement for Semiconductor Materials

2.1 Resistivity 6
2.2 Carrier Lifetime 9
2.3 Inhomogeneities 11
2.4 Infrared Methods 15
2.5 Hall Effect 16
2.6 Gold-Doped Silicon 16
2.7 Specification of Germanium 17
2.8 References 21

3. Methods of Measurement for Semiconductor Process Control

3.1 Metallization Evaluation 23
3.2 Processing Facility 28
3.3 Die Attachment Evaluation 31
3.4 Wire Bond Evaluation 31
3.5 References 46

4. Methods of Measurement for Semiconductor Devices

4.1 Thermal Properties of Devices 48
4.2 Thermographic Measurements 51
4.3 Microwave Device Measurements 51
4.4 Silicon Nuclear Radiation Detectors 52
4.5 References 54

Appendix A. Joint Program Staff 55

Appendix B. Standards Committee Activities 56

Appendix C. Solid-State Technology and Fabrication Services 57

Appendix D. Joint Program Publications 58

LIST OF FIGURES

PAGE

1. Resistivity profiles along a diameter of an *n*-type germanium, thin, circular wafer obtained by the four-probe and photovoltaic methods 14

2. Resistivity profiles along a diameter of a *p*-type germanium, thin, circular wafer obtained by the two-probe, four-probe, and photovoltaic methods 14

3. Nomograph relating the time t, temperature T, applied bias V, and drifted depth W 18

4. Gamma-ray peak shapes for ^{137}Cs 18

5. Scratch test apparatus 24

6. Test data for the determination of threshold adhesion failure obtained from a set of typical scratch test measurements 26

7. SEM photomicrophotographs of stylus tips 27

8. The sequence of producing a mask set 30

9. A section of the diode array produced by the mask set 30

10. Mechanical resonance curves taken on the same transducer driven by three different ultrasonic power supplies 32

11. Vibration amplitude of an ultrasonic bonding tool 32

12. Modification of transducer horn to reduce the mechanical Q 34

13. Response of the bonding tool vibration amplitude to frequency modulation of the power supply oscillator 36

14. Wire marks in the coating of a spool left by 0.00 1-in. diameter aluminum bonding wire 38

15. Pull strength in grams as a function of bonder power setting for oxidized substrate, aluminum sintered at 550°C 38

16. SEM photomicrographs (575 X) of aluminum ultrasonic wire bonds showing heel crack and clamp marks 40

17. SEM photomicrographs (460 X) of bond adhesion (lift-off) patterns for first bonds made at different time settings and constant power setting 42

18. SEM photomicrograph (800 X) of bond adhesion (lift-off) pattern for a strong first bond 44

19. SEM photomicrographs (600 X) of bond adhesion (lift-off) patterns for two second bonds made consecutively at identical time and power settings 44

20. Block diagram of apparatus used to generate and plot curves of the temperature difference between the device junction and the case as a function of collector-emitter voltage with the collector current held constant 49

LIST OF TABLES

1. Doping mixture flow rates 30

METHODS OF MEASUREMENT FOR SEMICONDUCTOR MATERIALS, PROCESS CONTROL, AND DEVICES

Quarterly Report
October 1 to December 31, 1969

ABSTRACT

This quarterly progress report, sixth of a series, describes NBS activities directed toward the development of methods of measurement for semiconductor materials, process control, and devices. Principal emphasis is placed on measurement of resistivity, carrier lifetime, and electrical inhomogeneities in semiconductor crystals; evaluation of wire bonds, metallization adhesion, and die attachment; and measurement of thermal properties of semiconductor devices and electrical properties of microwave devices. Work on related projects on silicon nuclear radiation detectors and specification of germanium for gamma-ray detectors is also described. Supplementary data concerning staff, standards committee activities, technical services, and publications are included as appendixes.

Key Words: Alpha detectors; aluminum wire; carrier lifetime; die attachment; electrical properties; epitaxial silicon; gamma detectors; germanium; gold-doped silicon; metallization; methods of measurement; microelectronics; microwave devices; nuclear radiation detectors; resistivity; semiconductor devices; semiconductor materials; semiconductor process control; silicon thermal resistance; thermographic measurements; ultrasonic bonder; wire bonds.

1. INTRODUCTION AND HIGHLIGHTS

This is the sixth quarterly report to the sponsors of the Joint Program on Methods of Measurement for Semiconductor Materials, Process Control, and Devices. The report is subdivided according to tasks which have been identified as parts of the Program. Section 2 deals with methods of measurement for materials; section 3, with methods of measurement for process control; and section 4, with methods of measurement for devices. Contrary to previous practice, references for a particular section are listed in a separate subsection at the end of that section.

Resistivity — Two new round-robin experiments involving the four-probe method for measuring resistivity are being coordinated at the request of ASTM Committee F-1. In the study of the dependence of four-probe

resistivity on current, probe force, and surface finish it was necessary to repeat some of the measurements on specimens with lapped surfaces before beginning work on specimens with polished surfaces. New equipment was designed and built for both the spreading resistance and capacitance-voltage methods in order to permit more detailed study of these methods.

Carrier Lifetime — Emphasis in the carrier lifetime task was placed on the study of methods for measuring carrier lifetime in epitaxial layers. Work is underway on both the metal-oxide-semiconductor capacitance and surface photovoltage methods for this measurement. Emphasis on measurement of carrier lifetime in diode structures has been shifted back to the study of the abrupt *p-n* junction in order to resolve the discrepancy between minority carrier lifetime values as measured by the voltage decay and reverse recovery techniques.

Inhomogeneities — The analysis of the photovoltaic method for measuring radial resistivity gradients in germanium and silicon circular wafers has been extended to include measurements made with knife-edge pressure contacts. Use of these contacts makes the application of the method to production monitoring much more attractive. Preliminary results suggest that the use of these contacts will be possible despite the fact that some difficulty has been encountered in measuring the photoconductivity near the contacts. A further advantage of this technique is that it permits the van der Pauw technique to be used to determine the average resistivity of the wafer, and the expression relating the resistivity gradient to the photovoltage has been modified to take this into account. The interest of the industry in the application of this method is being sought.

Other Measurement Methods for Materials — Work on the development of infrared methods is drawing to a close. A summary report has been prepared to describe the work on oxygen determination by infrared absorption. An informal report on the use of low temperature photoconductivity for identifying and determining the concentration of deep-lying impurities in silicon and germanium is being prepared.

During this quarter no work was carried out on either the high field effects task or the deep-level studies task. Work on the former has been suspended indefinitely in order that the staff originally assigned part time to it may devote all their efforts to the wire bond evaluation task. Work on the latter will be completed before the end of this fiscal year.

Metallization Evaluation — Studies of the scratch test for determining adhesion strength of aluminum films has led to the development of a new concept, threshold adhesion failure, as a criterion for evaluating the result of the test. This concept involves the identification of the load at which any removal of the film can be detected rather than complete removal as required by the previous critical load criterion. The

importance of the nature of the stylus tip to this test has led to detailed study of the topography of the tip both by shadowgraph techniques and with the scanning electron microscope.

Wire Bond Evaluation — Further progress was made in the characterization of the ultrasonic bonding system by means of the capacitor microphone technique. Mechanical resonance curves were measured on the same transducer-tool combination, driven successively by three different commercial ultrasonic power supplies. As predicted from earlier measurements made with special laboratory amplifiers, the mechanical Q was lowest in the case of constant current drive and highest in the case of constant voltage drive. Further experiments demonstrated that the mechanical Q of a system driven by a constant-power source can be reduced by drilling an array of holes in the transducer horn. A low-Q system is desirable because the detuning effects of thermal environmental changes and instabilities in the oscillator are reduced.

Another way of minimizing the effect of resonant frequency shifts is with the use of swept-frequency operation. Detailed studies of such operation were made for a constant-power source swept by various modulation voltage wave forms.

These studies of bonder characteristics are an essential feature of the development of a process which will yield the reproducible bonds necessary for evaluation of the pull and other tests for bond strength. They also yield information of immediate value to suppliers and to users of the equipment, such as those producing devices for one of the sponsors of the Joint Program. During this quarter, considerable effort was directed toward identification of problems encountered on operational lines.

Extensive use was made of the scanning electron microscope for studying bonds made both on commercial lines and in-house. Detailed studies were made on the bonding pattern by observing the bonding pad after the bond had been peeled off.

Preparation of both the bibliography and critical review survey paper on wire bond evaluation is continuing.

Other Measurement Methods for Process Control — Work is continuing on development of the processing facility and in the study of die attachment evaluation. Additional assistance was given ASTM Committee F-1 in the development of standard procedures for leak testing. The correlation of NASA test methods, ASTM test methods, and the requirements of NASA line certification was initiated. This work has taken on broader significance since the NASA line certification requirements are cited in the General Specification for Microcircuits, MIL-M-38510. Their use is mandatory for class A microcircuits.

Measurement Methods for Devices — Further measurements of d-c current gain as a function of collector-emitter voltage were made on a variety of transistor structures in the investigation of the applicability of this measurement as a screen for devices susceptible to hot-spot formation. The apparatus for measuring thermal resistance by the emitter-base voltage technique as a function of collector-emitter voltage has been partially automated.

In the area of second breakdown measurement, continuing assistance is being given to JEDEC Committee JS-6 on Power Transistors in regard to definitions of second breakdown and the writing of "Users Guide to Power Transistors."

Work on microwave device measurements was expanded significantly with the addition of a full-time senior staff member on this task. Assembly of experimental equipment for measurement of mixer diode noise parameters at X band was begun.

Symposia — Arrangements for the Symposium on Silicon Device Processing to be held in June, 1970, under the joint sponsorship of ASTM Committee F-1 and the National Bureau of Standards are continuing as planned. Final selection of the papers to be presented in the various sessions is to be made early in 1970. At the request of one of the sponsors, organization of a limited-attendance information exchange on problems associated with ultrasonic wire bonds is being considered.

History and Sponsorship — The Joint Program was undertaken last year to focus NBS efforts to enhance the performance, interchangeability, and reliability of discrete semiconductor devices and integrated circuits through improvements in methods of measurement for use in specifying materials and devices and in control of device fabrication processes. These improvements are intended to lead to a set of measurement methods which have been carefully evaluated for technical adequacy, which are acceptable to both users and suppliers, and which can provide a common basis for the purchase specifications of government agencies. In addition, such methods will provide a basis for controlled improvements in essential device characteristics, such as uniformity of response to radiation effects. The Program is supported by the National Bureau of Standards,† the National Aeronautics and Space Administration,* the Defense Atomic Support Agency,× and the U. S. Navy Strategic Systems Project Office.§ Because of the cooperative nature of the Program, there is

---

† Through Research and Technical Services Projects 4251120, 4251123, 4251126, 4252128, 4254111, 4254112, and 4254115.

* Through Order ER-22448, Electronics Research Center. (NBS Project 4251523)

× Through Project Order 808-70. (NBS Project 4259522)

§ Administered by U. S. Naval Ammunition Depot, Crane, Indiana through Project Orders PO-0-0036 and PO-0-0055. (NBS Project 4259533)

not a one-to-one correspondence between the tasks described in this report and the projects by which the Program is supported. Although all sponsors subscribe to the need for the entire basic program for improvement of measurement methods for semiconductor materials, process control, and devices, the concern of certain sponsors with specific parts of the Program is taken into consideration in planning.

Additional background information on the Program and individual tasks may be found in earlier reports in this series (see Appendix D). Besides the tasks sponsored under the Joint Program, this report contains descriptions of activity on related projects supported by NBS or other agencies. Although the specific objectives of these projects are different from those of the Joint Program, much of the activity undertaken in these projects will be of interest to Joint Program sponsors. The sponsor of each of these related projects is identified in the description of the project.

2.1 RESISTIVITY

Objective: To develop improved methods, suitable for use throughout the electronics industry, for measuring resistivity of bulk, epitaxial, and diffused silicon wafers.

Progress: Work has continued on programs to improve understanding and control of the factors which limit the precision and accuracy of the four-probe resistivity measurement technique and to extend its range of applicability to specimens with higher resistivity, polished surfaces, or thin layers. Two alternative techniques, spreading resistance and capacitance-voltage, which are particularly useful for measuring resistivity and resistivity profiles on thin-layer structures are being studied to determine the parameters which limit their effectiveness and intercomparability.

Four-Probe Method — Two round-robin experiments are being coordinated in conjunction with ASTM Committee F-1. The first is to establish the precision which can be expected from the four-probe method [1] when it is used to measure silicon wafers with room temperature resistivity up to 10,000 Ω-cm. Detailed resistivity profiles were taken of the material available for this round robin, both to select the most uniform slices for consideration and to have more detailed information with which to correlate any anomalies which may occur in the round robin results. Measurements made indicated that enough satisfactory wafers were available, and selected wafers were mailed to the first participant. In addition, single laboratory precision figures were obtained at the slice centers for the slices considered. The relative sample standard deviation was ±1.5 percent or less of the average value for each slice measured. During the course of these measurements it was found that electrical guarding of the potential-measurement leads resulted in considerable reduction of background noise and, hence, improvement in short-term stability [2].

In the other round robin, the four-probe method is used to measure the resistivity of silicon epitaxial layers deposited on substrates of the opposite conductivity type. Material to be included in this round robin has been measured according to a draft procedure derived from the standard method for making four-probe resistivity measurements on wafers [1]. Three of the epitaxial slices, although showing no severe measurement difficulty, did have enough surface damage that they could not be used for the round robin.

The study of the dependence of four-probe resistivity measurement on current, probe force, and surface finish has continued. Because of inconsistencies in the data collected to date, the silicon wafers under

study, which cover each decade in the resistivity range 0.001 to 100 Ω-cm, were remeasured. The surfaces were freshly lapped with 5-μm alumina and thoroughly washed prior to remeasurement. Measurements with probe loading of 150 g have been completed for a two-decade current range about the recommended value [1] for these wafers. The wafers in general show a nearly flat current dependence; all but two wafers show less than a 1-percent change in resistivity between the lowest and highest currents used. A slightly higher resistivity value at the lowest current is a general feature. This study is being continued with determination of the current dependence of the resistivity of these wafers at lower probe loadings on the same 5-μm lapped surfaces.

(F. H. Brewer, J. R. Ehrstein, and D. R. Ricks)

Spreading Resistance Methods — This technique is widely used for depth profiling of both diffused and epitaxial structures and can also be used for radial profiling of both wafers and thin layers because of its applicability to regions of either conductivity type over a seven-decade range of doping densities. Lack of correlation of results among several variants of the technique appears to be due to lack of a full understanding of the degree of control required for the experimental variables. This was evidenced by the results of a preliminary round robin which was undertaken by ASTM Committee F-1.

As part of a study of the effect of various parameters on this measurement a new probe holder was designed and built. The design of this holder allows control of the probe position on the wafer surface, repeatability of probe loading to within better than 0.25 g in the total load range from 10 to 50 g, and regulation of the probe impact velocity to values as low as 0.1 mm/s. These features allow the attainment of reproducible contact between the probe and the wafer. Further efforts were made to reduce the electrical noise in the measurement circuit. At present, measurements can be made with 10-μV sensitivity for silicon in all resistivity ranges and with somewhat improved sensitivity for silicon with resistivity less than 1 Ω-cm. (J. R. Ehrstein)

Capacitance-Voltage Method — This method utilizes the measurement of capacitance as a function of bias voltage applied to a junction in a semiconductor wafer or epitaxial layer to yield a measure of the doping density as a function of depth into the wafer. It has a primary position among impurity density and hence resistivity measurements, in that it is the only technique applicable to thin layers on conducting substrates which does not rely on a transfer calibration from some other measurement. With the aid of a digital computer, the data are fitted to a theory based on an approximate model for the junction to obtain values of carrier density versus diode depletion depth. Although the method is relatively more time consuming than either the spreading resistance and four-probe methods and has definite limitations with regard to the range of layer thickness which can be probed, it is of great importance as a reference

method with which to compare the results of other resistivity measurements on thin layers. This method is being studied to gain a better understanding of the conditions which affect its precision and limitations both to make it useful as a technique with which to compare the results of four-probe and spreading resistance measurements, also under study, and to provide measurement capability useful to other in-house programs.

A semiautomated data taking system has been assembled to expedite the measurement of capacitance as a function of bias voltage on these diodes. Interface circuitry was designed and built so the outputs of direct-reading capacitance and voltage meters can be recorded by an operational data acquisition system which consists of a scanner, digital voltmeter, and card-punch. At present bias voltages must be selected manually. However a fully automatic sequencing system for this bias voltage has been designed and is being built. The investigation of planar diodes with this technique has been slowed by difficulties in diode fabrication which have now been resolved. (G. N. Stenbakken)

Plans: The investigation of the current and probe-force dependence of resistivity as measured by the four-probe method on lapped wafer surfaces will be completed and studies of wafers with mechanically and chemically polished surfaces will begin.

Three new specimens for the four-probe epitaxial silicon resistivity round robin will be obtained, and the set will be sent to the first participant. Data will be reduced and tabulated as received from participants in this and the four-probe high resistivity silicon wafer round robin.

In the next phase of the spreading resistance investigation, the measurement will be studied at various values of current and probe force. To minimize the number of variables to be controlled, measurements will be made with a single spreading resistance contact on wafers with a large area back contact. Initial measurements will be on silicon wafers in the resistivity range 0.1 to 10 Ω-cm. Wafers with both lapped and mechanically polished surfaces will be studied. Osmium and tungsten carbide will be used as probe tips.

Capacitance-voltage measurements will be made on both planar and mesa diodes fabricated on bulk silicon wafers. These measurements will be used to identify and study the important factors which affect the precision and accuracy of this method.

2.2 CARRIER LIFETIME

Objective: To determine the fundamental limitations on the precision and applicability of the photoconductive decay method for measuring minority carrier lifetime and to develop alternate methods for measuring minority carrier lifetime in germanium and silicon which are more precise, more convenient, or more meaningful in the specification of material for device purposes.

Progress: Effort on the carrier lifetime task has continued in the four areas established last quarter (NBS Tech. Note 520, pp. 13-16). In the area of bulk crystal measurements, the study designed to establish the single-laboratory precision to be expected from the revised photoconductive decay (PCD) method has been initiated, and additional surface photovoltage (SPV) measurements have been made on the specimens in the intercomparison study. Study of both the metal-oxide-semiconductor (MOS) capacitance and SPV methods for measurement of carrier lifetime in epitaxial layers is continuing. Emphasis in the diode area has been shifted back to the study of the abrupt *p-n* junction diode in order to resolve the discrepency between minority carrier lifetime values as measured by the voltage decay and reverse recovery techniques. The study of methods for measuring minority carrier lifetimes in transistor structure, still in its preliminary stages, did not progress significantly.

Bulk Crystals — The experiment to establish a multi-operator, single-laboratory precision for the revised procedure for carrier lifetime measurement by the PCD method was begun. The first operator has completed measurements on five specimens. It has become evident that, in addition to its primary purpose, this experiment will also yield suggestions from the various operators that will assist in improving the form of the revised procedure. (R. L. Mattis and F. R. Kelly)

Carrier lifetime was measured by the SPV method on six silicon and two germanium specimens which had been previously measured by the PCD method. In several cases there was substantial disagreement between the SPV and PCD values. It is not yet clear whether these differences are real or if they result from problems with the SPV measurement. The SPV measurement is being repeated on some specimens on which the surface recombination velocity has been reduced in an effort to resolve the question. (H. A. Gitelson and W. E. Phillips)

Epitaxial Layers — The review of the published literature on MOS capacitance measurements was completed. Several ways were found to deduce the minority carrier lifetime from the transient change in MOS capacitance which follows a change in the applied voltage. Jund and Poirier [1] derive the lifetime in epitaxial layers from the transient increase in capacitance following the application of a voltage step with the assumption that this transient is exponential. Heiman [2] is able to deduce the lifetime from a non-exponential capacitance change. Zerbst [3] obtains a straight line when he plots the time derivative of the

square of the reciprocal capacitance against the reciprocal capacitance. The slope of this line is proportional to the lifetime and the intercept on the ordinate is proportional to the surface recombination velocity. Tomanek [4] describes a method in which an MOS capacitor is biased into inversion after which pulses of opposite polarity and variable duration are applied. The values of capacitance measured just as the pulse is terminated for various duration times are used to determine the carrier lifetime.

To proceed further it is necessary to demonstrate the equivalence of these various approaches either theoretically, experimentally, or both or to confirm the validity of one or more nonequivalent approaches. Before starting this relatively complex study, a survey to determine the extent of use of MOS capacitance measurements of lifetime in the industry has been initiated. (R. L. Mattis)

The theoretical analysis of the SPV response when the condition that the diffusion length be less than the thickness of the specimen is violated indicated that a plot of photon intensity against penetration depth, or reciprocal absorption coefficient, should yield a straight line for penetration depths greater than the surface depletion depth. This finding is in accord with experimental results reported last quarter. However, the intercept of this line extrapolated to zero photon intensity was found to be dependent on the thickness of the specimen as well as the diffusion length. This result may be also applied to interpret SPV measurements in thin epitaxial layers since the SPV response in such layers can be treated in the same manner as a thin specimen with very large surface recombination velocity on the back surface. Further analysis is underway to determine whether or not the value of diffusion length can be extracted from SPV measurements on relatively thin layers of known thickness. (W. E. Phillips)

Diodes — Emphasis in this area has been shifted back to the study of the abrupt p-n junction diode with the aim of resolving the discrepancy between the values of minority carrier lifetime measured by means of the voltage decay and reverse recovery techniques. Theoretical study revealed no basis for this difference. Examination of the experimental conditions used in previous measurements has shown that these measurements were made at substantially different current levels. Both the voltage decay and reverse recovery circuits are being modified so that these measurements can be repeated at the same current levels.

An experiment to determine the reproducibility to be expected from the reverse recovery measurement on a single-operator basis has been conducted over a six-month period. The reverse recovery time of seven commercial diodes was measured at intervals throughout the course of the experiment. Equal forward and reverse currents of 4 mA were employed. The diodes were driven by a square wave generator at a frequency of 1 kHz.

The effective lifetime was calculated as 4.4 times the measured recovery time (the time between the current zero and the beginning of current decay, see NBS Tech. Note 475, pp. 6-7). Standard deviations ranging from 4 to 13 percent were observed. (A. J. Baroody)

Transistors — Study of literature on methods for measuring minority carrier lifetime in transistor structures was deferred pending completion of the analysis of SPV response. (W. E. Phillips)

Plans: Work on the PCD method will continue with emphasis on the establishment of the single-laboratory, multi-operator precision. A number of SPV measurements will be repeated as part of the intercomparison study between the SPV and PCD methods.

Guided by the extent of industry usage, a decision will be made concerning the continuation of the study of the MOS capacitance technique for measuring minority carrier lifetime. If the study is continued, the various approaches referenced above will be examined both theoretically and experimentally to determine the extent of their equivalance. Analysis of the SPV method will continue in order to determine the suitability for measurement of minority carrier lifetime in thin epitaxial layers.

After modifications to the voltage decay and reverse recovery circuits are completed, experimental work will resume on the study of the dependence of carrier lifetime on current level and frequency. The limits of applicability of the two techniques will be studied on commercial diodes which have been characterized by the capacitance-voltage technique to insure that they have abrupt junctions.

Review and study of methods for measuring carrier lifetime in transistor structures will resume.

2.3 INHOMOGENEITIES

Objective: To develop improved methods for measuring inhomogeneities responsible for reducing performance and reliability of germanium and silicon devices and, in particular, to evaluate a photovoltaic method as a means for measuring radial resistivity gradients in germanium and silicon circular wafers.

Progress: The evaluation of the relationship between photovoltage and radial resistivity gradients in germanium and silicon circular wafers was extended to include photovoltaic measurements made with knife-edge contacts rather than the specially prepared, semicircular, soldered contacts which have been used previously. A new specimen holder was designed and constructed to allow four knife-edge contacts to be made at

the ends of two orthogonal diameters of the specimen. In addition to permitting inhomogeneity measurements to be made along perpendicular diameters, this configuration also allows the measurement of the average resistivity of the specimen by the van der Pauw method [1, 2].

Use of the knife-edge contacts makes the application of the method to production monitoring much more attractive. Preliminary results indicate that it is possible to make the photovoltaic measurement, but some difficulty has been encountered in measuring the photoinduced change in resistance which must also be determined in order to evaluate the degree of inhomogeneity. With the knife-edge contacts, the measured value of the photoinduced change in resistance depends somewhat on the polarity of the current through the specimen; this dependence increases as the light probe approaches a contact. The difficulty is particularly pronounced in silicon wafers.

The derivation of the equation relating the photovoltage to the resistivity gradient along the diameter of the circular wafer was reexamined because it appeared that discrepancies between the resistivity profile obtained from photovoltaic and four-probe measurements were too large to be accounted for by the errors present in the methods.† It was found that a factor of 2 had been omitted in the previous derivation so that the resistivity gradient is actually twice as large as heretofore thought. At the same time the relation was modified to permit use of average resistivity as determined by the van der Pauw technique instead of the specimen resistance measured between contacts of known dimensions at the ends of the measurement diameter. The corrected and modified expression for the resistivity gradient, $d\rho/dx$, is as follows:

$$\frac{d\rho}{dx} = \frac{3}{2\pi} \times \frac{B}{1-(y/r)^2} \times \frac{\rho^2}{rt} \times \frac{V}{\Delta R}$$

where:

$B = \frac{q}{2KT}(1 + b)$,
q = charge of the majority carrier (C),
k = Boltzmann's constant (J/K),
T = absolute temperature (K),
b = ratio of the mobility of the majority carrier to the mobility of the minority carrier,
y = distance of light spot from specimen center (cm),
r = specimen radius (cm),

---

† This work was carried out with the assistance of Dr. L. J. Swartzendruber of the NBS Alloy Physics Section.

t = specimen thickness (cm),
ρ = average resistivity of the specimen (Ω-cm),
V = photovoltage (V), and
ΔR = photoinduced change in resistance of the wafer (Ω).

Use of the corrected equation has, in all cases, improved the agreement between the resistivity profiles determined from photovoltaic and four-probe measurements. Examples of the degree of agreement which can now be achieved are shown in Figs. 1 and 2. Significant differences still appear near the edge of the wafer, particularly in specimens such as the *p*-type germanium wafer shown in Fig. 2. Some of the differences in shape between the four-probe profile and the other two profiles of Fig. 2 arise because the spatial resolution of the four-probe method is limited by a characteristic distance somewhat larger than the 1.6-mm probe spacing used for both the two- and four-probe measurements. The resolution of the photovoltaic method is limited by the light probe diameter and the minority carrier diffusion length. For the above specimens, the volume sampled is approximately equal to that sampled by the two-probe method. Probe measurements were made every 1.25 mm. Photovoltage and photoconductivity data were averaged over 0.625-mm intervals and summed to obtain the resistivity as a function of position.

Expressions of interest in use of the photovoltaic method to determine radial resistivity variations were sought from a number of silicon and germanium suppliers through telephone contacts. Each contacted expressed positive interest particularly in the possible use of the method for measuring higher resistivity material intended for non-epitaxial, high-voltage devices and low-resistivity material intended for voltage-reference diodes. The potential of the method for making precise, continuous, contactless measurement of the resistivity gradient elicited particular attention. At present, radial resistivity gradients are measured almost exclusively by the four-probe method. To varying degrees the problems of each supplier with this method center around the lack of sufficient precision and the specimen damage which results from contacting the regions being measured.

Two additional applications arose as a result of the measurement needs expressed by the suppliers contacted. It was suggested that the contactless feature of the method could be exploited in the characterization and identification of polished specimens without the risk of degrading the surface. Currently this presents a serious measurement problem not only to the vendor but also to the user who wishes to determine that specimens conform to his specifications. Two suppliers were particularly interested in the possibility of using the method to measure longitudinal resistivity variations in as-grown semiconductor crystals. This is made difficult by the necessity for the light probe to generate electron-hole pairs uniformly throughout a narrow slice of the crystal; penetration depths from 2 to 8 cm are required.

(D. L. Blackburn and H. A. Schafft)

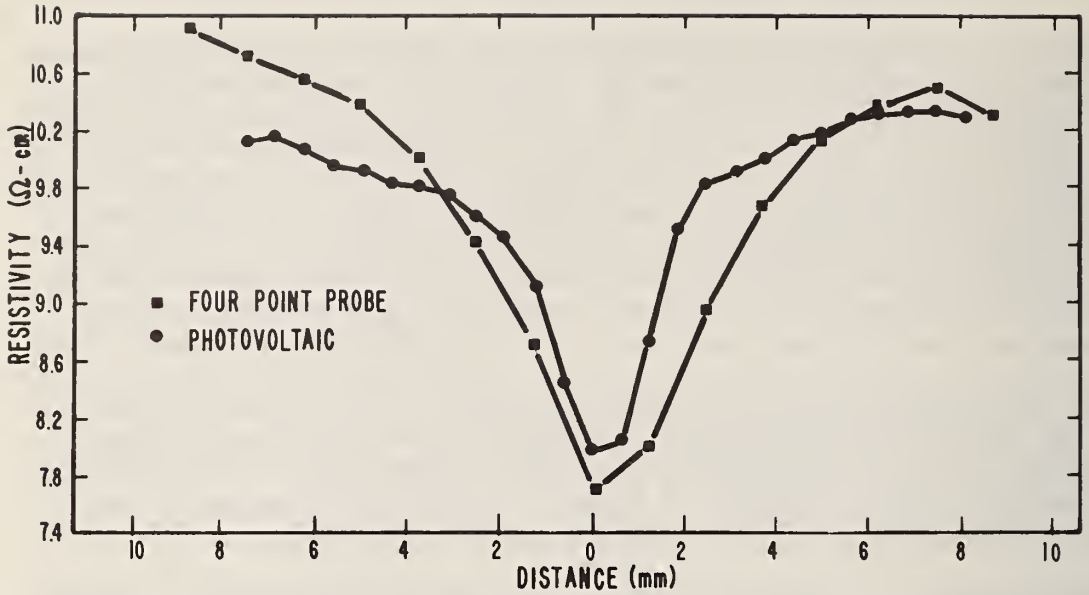

Fig. 1 Resistivity profiles along a diameter of an *n*-type germanium, thin, circular wafer obtained by the four-probe and photovoltaic methods. The diameter of the specimen was 22.4 mm.

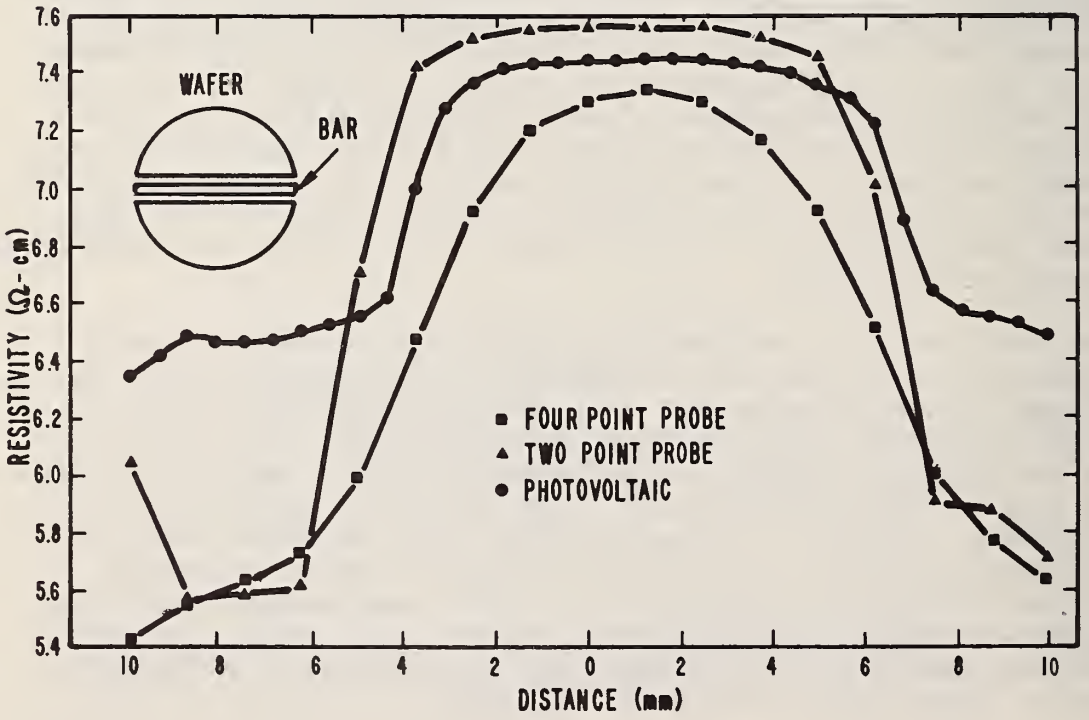

Fig. 2 Resistivity profiles along a diameter of a *p*-type germanium, thin, circular wafer obtained by the two-probe, four-probe, and photovoltaic methods. The two-probe resistivity profile was obtained on a narrow, bar-shaped specimen cut from the wafer as shown in the inset. The diameter of the circular wafer was 22.9 mm.

Plans: The relationship between photovoltage and radial resistivity gradient will be evaluated experimentally by determining how well resistivity profiles generated by this relationship, using data obtained both with special, relatively large area, contacts and with knife-edge contacts, compare both in shape and magnitude with profiles obtained with the two-probe method. Several specimens will be examined which exhibit the different but typical resistivity profile shapes that have been encountered. These specimens have already been chosen on the basis of the profiles obtained with four-probe measurements. Photovoltaic measurements will be made on at least one polished specimen to determine the feasibility of applying this method to such specimens.

Inquiry into the interest of semiconductor suppliers and users in the application of this method will continue.

2.4 INFRARED METHODS

Objective: To evaluate impurity photoconductivity as a method for detecting low concentrations of deep-lying impurities such as copper, gold, iron, and nickel in silicon and germanium, and to assist ASTM Committee F-1 in extending the applicability of infrared absorption as a method for detecting impurities such as oxygen and carbon in silicon and germanium.

Progress: A draft of the summary report [1] describing work completed on the determination of oxygen in silicon and germanium by infrared absorption methods has been written. An important part of this report is a comparison of the oxygen concentration deduced from absorption measurements made by various techniques on silicon specimens. In addition, results of measurements on both silicon and germanium at room temperature, 80 K, and 20 K are compared.

Assistance to ASTM Committee F-1 on the work on infrared absorption measurement methods was completed with a detailed review of the draft documents [2] submitted for committee letter ballot after the September meeting. Additional measurements at low temperatures have been made in conjunction with round-robin tests which are still being conducted by the committee.

Work continued on an informal report on the use of low-temperature photoconductivity (LTPC) for identifying deep-lying impurities and determining their concentration in silicon and germanium. The facility for making LTPC measurements has been modified so that infrared response (IRR) measurements on lithium-drifted germanium diodes (see Section 2.7) can also be made. (W. R. Thurber)

Plans: Work on oxygen determination by infrared absorption will be concluded with the publication of the summary report.

LTPC and IRR measurements will be made in connection with the task on Specification of Germanium and will be reported there. On completion of the informal report on LTPC measurements, the task on Infrared Methods will be terminated.

2.5 HALL EFFECT

Objective: To establish a facility for making measurements of Hall coefficient as a function of temperature between 4 and 350 K and to improve methods for collecting and interpreting Hall effect data.

Progress: Tests were made on the modified Hall effect apparatus which enables measurements to be made on high-resistivity specimens with the automatic data acquisition system. Preliminary observations indicated that the objectives of impedance matching and reduction of measurement time were realized. Minor changes were made to eliminate the effect of electrical leakage in the scanner circuit of the data acquisition system. (W. R. Thurber)

Work on the report concerning Hall effect measurements and their interpretation was deferred.

Plans: Detailed tests will be made with high-resistance resistors to determine how accurately specimens with resistance greater than 1 MΩ can be measured. Time constants associated with such measurements will also be determined.

Work will resume on the report concerning Hall effect measurements and their interpretation.

2.6 GOLD-DOPED SILICON

Objective: To characterize *n*- and *p*-type silicon doped with gold and to develop a model for the energy level structure of gold-doped silicon which is suitable for use in predicting its characteristics.

Progress: Initial electrical measurements were completed on 10 Ω-cm boron-doped silicon wafers which had been diffused with gold at temperatures of 850, 950, 1050, 1150, and 1250°C. It was found that the room temperature resistivity increased monotonically as the gold concentration, determined by neutron activation analysis, increased. This is contrary

to previous experimental observations but is in accord with theoretical calculations completed in the last quarter (NBS Tech. Note 520, p. 23). This suggests that the previously observed maximum in resistivity with increasing gold concentration may be an experimental artifact.

The gold concentration measured by neutron activation analysis techniques was in general lower than the solid solubility limit at the temperature of diffusion. To establish that this did not arise because of too short a diffusion time, two sets of 10 Ω-cm boron-doped silicon wafers were diffused with gold for various times. Times ranging from 30 min to 810 min were used for diffusion at 850°C while times from 15 min to 120 min were used at 1250°C. A section was cut from each wafer and lapped so that the gold concentration in the interior of the wafer can be determined by neutron activation analysis.

Slices from 0.1 and 1.0 Ω-cm *n*- and *p*-type silicon crystals have been cut in anticipation of additional gold diffusions. Further diffusions have been defered, however, until the discrepancy noted above is resolved. (W. M. Bullis and W. R. Thurber)

Plans: Gold diffusions and electrical measurements on the 1.0 and 0.1 Ω-cm wafers will be made after the discrepancy in gold concentration has been resolved.

2.7 SPECIFICATION OF GERMANIUM†

Objective: To measure the properties of germanium crystals and to correlate these properties with the performance of germanium gamma-ray detectors in order to develop methods for the early identification of crystals suitable for fabrication into lithium-compensated gamma-ray detectors.

Progress: Construction of the series of six nomographs relating to Ge(Li) detector technology has been completed, and the characterization of *p*-type, germanium single-crystals by observation of etch-pit distributions has begun. Gamma-ray pulse-height spectra have been obtained as a function of Ge(Li) detector bias in order to study empirically the change in peak shape with increased trapping of charge carriers. Various theoretical models which seek to predict peak shapes on the basis of trapping parameters were evaluated against experimental data.

---

† Supported by the Division of Biology and Medicine, U. S. Atomic Energy Commission. (NBS Project 4259425)

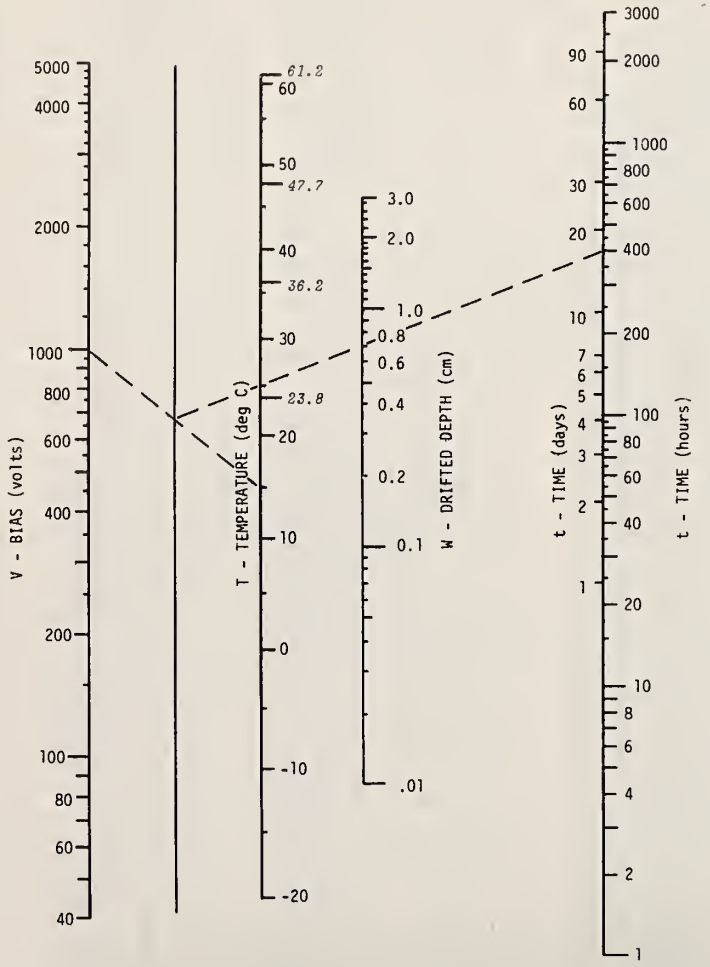

Fig. 3 Nomograph relating the time t, temperature T, applied bias V, and drifted depth W. For example, at 15°C and 1000 V applied bias, W is 0.8 cm after a drift time of 400 hours if the drift follows the equation: $W = (2\mu Vt)^{1/2}$

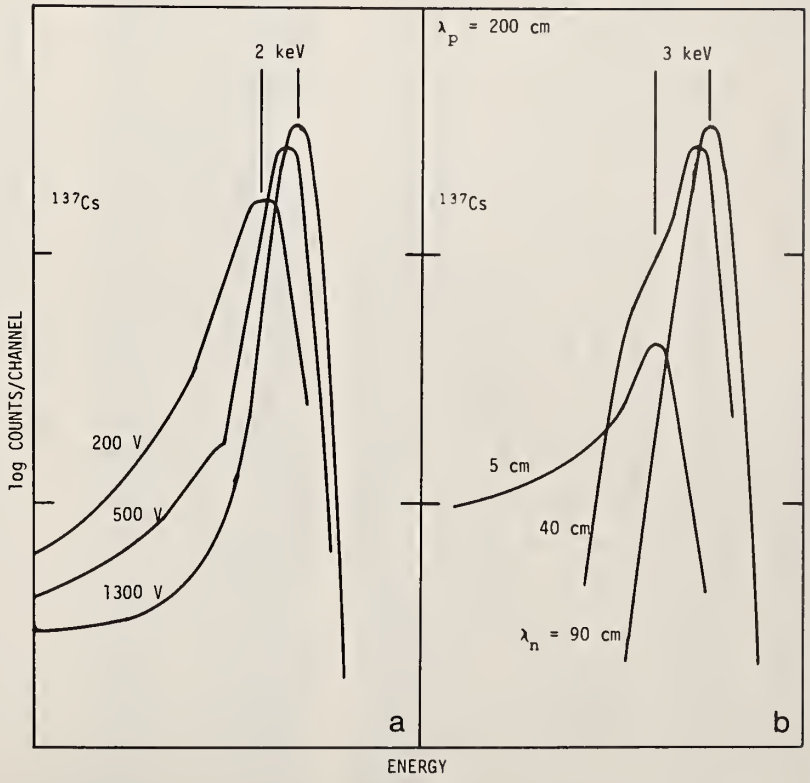

Fig. 4 Gamma-ray peak shapes for ^{137}Cs.
a: Experimentally obtained from Ge(Li) detector as a function of bias.
b: Theoretically calculated peak shapes [5] as a function of electron trapping length, λ_n.

Nomographs for Ge(Li) Detector Technology — Preparation of the series of nomographs relating to the fabrication and testing of Ge(Li) detectors has been completed with the development of a nomograph relating the area, drifted depth, and capacitance for right-circular cylindrical, double-open-ended, true coaxial Ge(Li) detectors. The nomograph for determining the drifted depth as a function of time, temperature, and applied bias during drift has been revised by combining the two charts previously required into a single alignment chart with five parallel scales as shown in Fig. 3. The relationship between oxygen concentration, acceptor impurity concentration, and lithium-ion drift mobility and the range of interest of these parameters makes it difficult to construct a single alignment chart such that the resulting scale calibrations are usuable over the range of interest. Therefore, the figure relating the above parameters will be retained in its present concurrency nomograph form (NBS Tech. Note 488, p. 17). Work has begun on text material containing directions for use, comments, and examples to accompany the series of six nomographs.

The equation used in constructing the nomograph relating the capacitance C (pF), junction area A (cm^2), and drifted depth W (cm) for planar Ge(Li) detectors was $C = 1.41\ (A/W)$. For true coaxial Ge(Li) detectors, the capacitance C (pF) is related to the detector length L (cm) and ratio of outer and inner radii R_2/R_1 (such that $R_2 - R_1$ is the drifted depth) by $C = 1.41\ (2\pi L)\ [\ln(R_2/R_1)]^{-1}$. The prefactor 1.41 pF/cm is the product of ε_0, the electrical permittivity of vacuum, and κ, the dielectric constant of germanium. Previously published values of the prefactor $\varepsilon_0\kappa$ erroneously give a value of 1.44 pF/cm [1, 2].

(A. H. Sher)

Characterization of Germanium — Approximately two-thirds of the crystals which had been assembled for characterization have been etched [3] to develop etch-pit patterns on the (111) faces. The crystals have been sorted with respect to the type of pattern found, such as star, ring, or propellor, for comparison with the results of infrared response (IRR) measurements on Ge(Li) structures [4]. Further testing of the low-noise preamplifier constructed for use with the IRR measurements was suspended when it was found that a commercial low-noise detector preamplifier was suitable for use in the measurement system.

(A. H. Sher, W. J. Keery, and H. E. Dyson)

Work has resumed on the paper comparing the measurement of oxygen concentration in germanium by the methods of lithium mobility, lithium precipitation, and infrared absorption. This paper includes a discussion of the range of applicability of each method as well as correlations between them. (A. H. Sher, W. K. Croll, and W. R. Thurber)

Ge(Li) Detector Measurements — Within the framework of the study of gamma-ray peak shapes obtained from pulse-height spectra using Ge(Li)

detectors, several theoretical models from which peak shapes can be predicted on the basis of carrier trapping parameters have been evaluated against experimental data. Figure 4a shows the change in peak shape of the ^{137}Cs, 662-keV gamma-ray spectrum as a function of applied bias for Ge(Li) detector 213.

Figure 4b shows peaks calculated from the model proposed by Trammel and Walter [5] for a gamma-ray of 662-keV energy, a detector of 8.5 mm drifted depth, and a fixed hole trapping length, λ_p, of 200 cm. The electron trapping length, λ_n, was varied from 90 to 5 cm to simulate increased electron trapping in the detector as the applied bias is reduced, but there is no direct correspondence between the variation in applied bias in the experimental case of Fig. 4a and the variation in λ_n in Fig. 4b. However, it is interesting to note that the model does predict a small shift downward in energy with increased carrier trapping as observed in the experimental case. The tailing observed on the low energy side of the peaks, however, does not grow from the base of the peak as seen in Fig. 4a, but from near the top of the peak. The ratio of the height of the peak to the height at the point at which the tail intersects the peak is also much smaller than observed in the experimental data.

One problem with this model as the authors themselves point out [5], is that the calculations are restricted to the case where there is a uniform probability of carrier trapping throughout the sensitive volume of the detector. This has been shown to be inconsistent with experimental results [6, 7]. Thus, while the model does predict relatively small shifts to lower energy of gamma-ray pulse-height peaks with increasing trapping of charge carriers as well as the magnitude of increase in peak width at half the maximum peak-height, it is not accurate enough for use in quantitative evaluation of trapping parameters from experimental data. Similar results are also obtained from a model proposed earlier by Chartrand and Malm [6].

The series of experimental spectra which is currently being obtained from Ge(Li) detector 213 as a function of applied bias are part of an empirical study of the variation in peak shape with increased carrier trapping being carried out in order to specify the characteristics of a theoretical model which would accurately reflect changes in the experimental data. (A. H. Sher and W. J. Keery)

Plans: Lithium mobility studies, Ge(Li) detector performance measurements, and the investigation of the relationship between etch-pit distributions on *p*-type germanium crystals and the characteristics of Ge(Li) detectors fabricated from the crystals will be continued. Impurity photoconductivity measurements will be made on germanium crystals which show a high degree of carrier trapping; measurements of infrared response will also be made at 77 K on Ge(Li) structures fabricated from this material.

2.8 REFERENCES

2.1 Resistivity

1. "Method of Test for Resistivity of Silicon Slices Using Four Pointed Probes" (ASTM Designation: F84-68T), *1969 Book of ASTM Standards*, Part 8, November, 1969. This document covers the range 0.05 to 120 Ω-cm; a revision covers the range 0.001 to 2000 Ω-cm.

2. A similar conclusion was reached on somewhat lower resistivity material by J. K. Hargreaves and D. Millard, "The Accuracy of Four-Probe Resistivity Measurements on Silicon," *Brit. J. Appl. Phys.* 13, 231-234 (1962).

2.2 Carrier Lifetime

1. C. Jund and R. Poirier, "Carrier Concentration and Minority Carrier Lifetime Measurement in Semiconductor Epitaxial Layers by the MOS Capacitance Method," *Solid-State Electronics* 9, 315-319 (1966).

2. F. P. Heiman, "On the Determination of Minority Carrier Lifetime From the Transient Response of an MOS Capacitor," *IEEE Trans. Electron Devices* ED-14, 781-784 (1967).

3. M. Zerbst, "Relaxationseffekte an Halbleiter-Isolator-Grenzflächen," *Z. Angew. Phys.* 22, 30-33 (1966).

4. P. Tomanek, "Measuring the Lifetime of Minority Carriers in MIS Structures," *Solid-State Electronics* 12, 301-303 (1969).

2.3 Inhomogeneities

1. Standard Method for Measuring Hall Mobility in Extrinsic Semiconductor Single Crystals (ASTM Designation: F76-68), *1969 Book of ASTM Standards*, Part 8, November, 1969.

2. L. J. van der Pauw, "A Method of Measuring Specific Resistivity and Hall Effect of Discs of Arbitrary Shape," *Philips Research Reports* 13, 1-9 (1958).

2.4 Infrared Methods

1. W. R. Thurber, "Determination of Oxygen in Silicon and Germanium by Infrared Absorption," NBS Tech. Note (in preparation).

2. Recommended Practices for Infrared Absorption Analysis of Impurities in Single Crystal Semiconductor Materials; Method of Test for Interstitial Oxygen Content of Silicon by Infrared Absorption; Method of Test for Interstitial Oxygen Content of Germanium by Infrared

Absorption; Method of Test for Substitutional Carbon Content of Silicon by Infrared Absorption.

2.7 Specification of Germanium

1. G. A. Armantrout, "A Fabrication Technique for Significantly Reducing the Capacitance of Large-Volume Ge LID Detectors," *IEEE Trans. Nucl. Sci.* NS-13, No. 3, 328-335 (1966).

2. D. Camp, "Application and Optimization of the Lithium-Drifted Germanium Detector System," UCRL-50156 (March 1, 1967), p. 10. (Available from the Clearinghouse for Federal Scientific and Technical Information (CFSTI), Springfield, Va. 22151)

3. W. L. Hansen, R. H. Pehl, E. J. Rivet, and F. S. Goulding, "Selection of Germanium for Lithium-Drifted Radiation Detectors by Observation of Etch-Pit Distributions," UCRL-19326 (October, 1969); to be published in *Nucl. Instr. & Meth.*

4. G. A. Armantrout, "A Highly Sensitive Photoresponse Technique for Determining Impurity and Defect Energies and Concentration in Germanium," presented at Third International Conference on Photoconductivity, Palo Alto, (August, 1969); UCRL-71625. (Available from CFSTI)

5. R. Trammel and F. J. Walter, "The Effects of Carrier Trapping in Semiconductor Gamma-Ray Spectrometers," *Nucl. Instr. & Meth.* 76, 317-321 (1969).

6. M. G. Chartrand and H. L. Malm, "Variation of the Gamma-Ray Resolution of Ge(Li) Detectors with the Position of Irradiation," AECL-2764 (June, 1967). (Available from Scientific Document Distribution Office, AECL, Chalk River, Ontario, Canada)

7. P. P. Webb, H. L. Malm, M. G. Chartrand, R. M. Green, E. Sakai, and I. L. Fowler, "Use of Collimated Gamma-Ray Beams in the Study of Ge(Li) Detectors," *Nucl. Instr. & Meth.* 63, 125-135 (1968).

3. METHODS OF MEASUREMENT FOR SEMICONDUCTOR PROCESSING

3.1 METALLIZATION EVALUATION

Objective: To improve methods for measuring the properties of thin film metal films with initial emphasis on adhesion of aluminum metallization deposited on various substrates.

Progress: As previously reported (NBS Tech. Note 520, pp. 27-29), familiarization studies had been made on the aluminum-quartz system using a rudimentary scratch test apparatus. This work, which broadly followed the method of Karnowsky and Estill [1], verified the suitability of this system for further detailed experiment. These efforts have been concentrated on evaluation of the test procedures and investigation of the topography of the stylus tips employed in the study.

Evaluation of the Scratch Test — A new scratch test apparatus was designed and built. This apparatus employs a balanced lever system as shown in Fig. 5. A commercial triple-beam balance is used to hold the specimen and supply a controlled stylus force (load) when balanced. The scribing stylus is held in a vertically adjustable jig so that it may contact the specimen while the beam apparatus is balanced. This jig is mounted on a heavy-duty stage which provides two orthogonal horizontal movements. With one movement the stylus is drawn across the specimen, while with the second the stylus is indexed laterally for subsequent scratches. The stylus track is observed through a microscope to detect film failure by transmitted light. The stylus load is continuously variable within the limits of the balance (0-1600 g) with a resolution of 0.1 g.

The criterion for adhesion failure has generally been considered to be complete removal of the film over a specified length (usually 1 cm) [1-4]. The stylus load required to do this is called the critical load. It was found in the familiarization studies that complete removal of the films over a 1 cm path is relatively infrequent. Moreover, private communications with earlier workers in this field revealed that under only the best experimental circumstances was complete removal "generally" achieved. Critical load determination, then, is often a matter of weighted judgement.

Because of the ambiguity of this criterion, the following operational definition was tentatively adopted for use in the present study:

> *threshold adhesion failure* occurs if, within the boundaries of a scratch and over its 1 cm path, removal of the film from its substrate can be detected by transmitted light with a microscope [magnification = 40 X] at even one spot no matter how small.

In addition, the following test conditions have been adopted:

(a) Aluminum film thickness: 0.5 μm,
(b) Substrate: fused quartz,

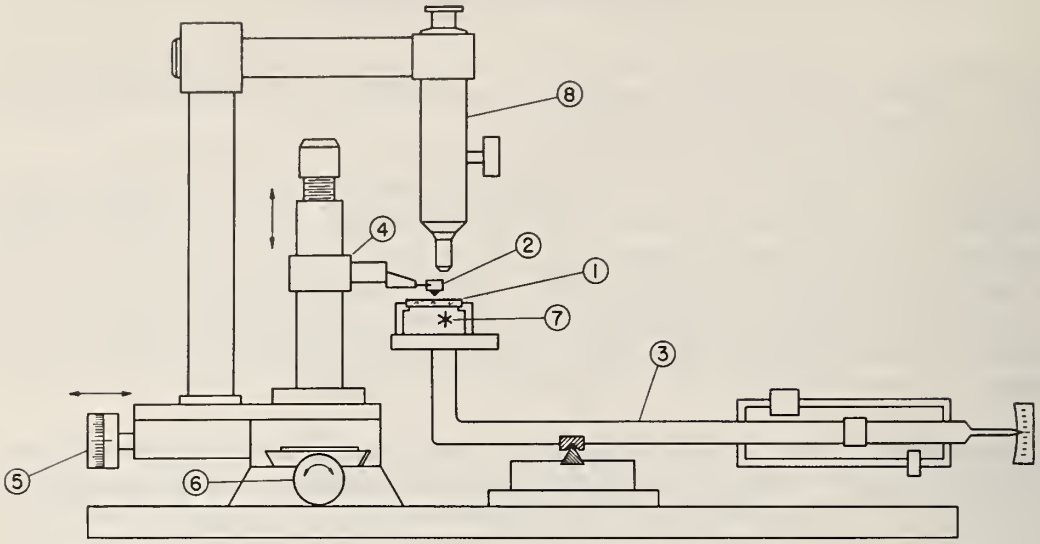

a: Schematic.

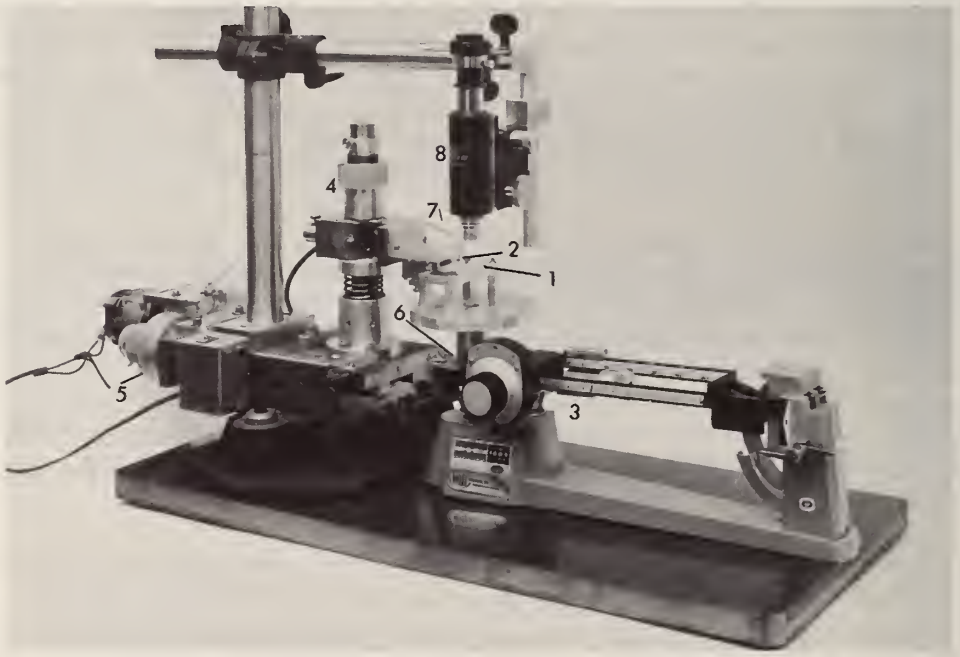

b: Photograph.

1. Specimen under test.
2. Stylus (in holder).
3. Triple-beam balance.
4. Vertical adjustment for stylus.
5. x-movement drive for scratching.
6. y-movement drive for indexing.
7. Fibre optic light source.
8. Viewing microscope.

Fig. 5 Scratch test apparatus.

(c) Stylus material: tungsten carbide or diamond,
(d) Stylus shape: right circular cone, 60-deg included angle, 50-μm nominal tip radius.

Initial tests with the new apparatus were conducted with a single tungsten carbide stylus. Films were prepared by vacuum evaporating aluminum of 99.999 percent purity on 75 mm by 25 mm by 1.5 mm transparent fused quartz sheets which had been cleaned and heat treated in air to remove adsorbed water [5] prior to the deposition of the film.

Three groups of measurements, one group in the central area and one group close to each end, were made on each of several films. For any group of test data, stylus load is plotted against scratch position. If threshold adhesion failure (response) is observed, it is plotted as V; if no failure (non-response), as o. Only one scratch is made at any stylus position; a second piece of meaningful data cannot be obtained by scribing over an existing scratch.

This type of data can be statistically analyzed conveniently if the up-and-down design [6] is used for the experiment. In this design the test is started at a level where about half of the scratches are expected to show threshold adhesion failure. The load is increased one increment after each non-response and decreased one increment after each response. Ideally, the load increment should be nearly equal to the standard deviation. For the initial tests, the load increment was taken as 0.1 g, the resolution of the balance.

A plot of a set of typical scratch test measurements on a freshly-deposited aluminum film in which the concept of threshold adhesion failure was applied is shown in Fig. 6. This and other measurements demonstrate that the scratch test can discriminate between loads 0.1 g apart. The precision of the test is limited by the resolution of the balance; statistical analysis [6] of the data suggests that the standard deviation in these measurements is actually somewhat smaller. In another experiment thirteen scratches were made with successively increasing (and then decreasing) loads to obtain complete removal of the film. At a load of 200 g complete removal was obtained on only one scratch. All scratches at lower ("massive") loads showed partial film removal in varying amounts, not necessarily in relative proportion to the applied load. On the basis of all experimental data gathered thus far, the ambiguity of the complete removal criterion and critical failure load is confirmed, and the concept of threshold adhesion failure from which a mean threshold failure load can be calculated statistically, appears sufficiently valid to investigate and develop in depth.

Stylus Tip Characteristics — A modified shadowgraph technique is currently being used to measure the overall radius of curvature of the stylus tips. A photomicrograph of the tip profile is made with a

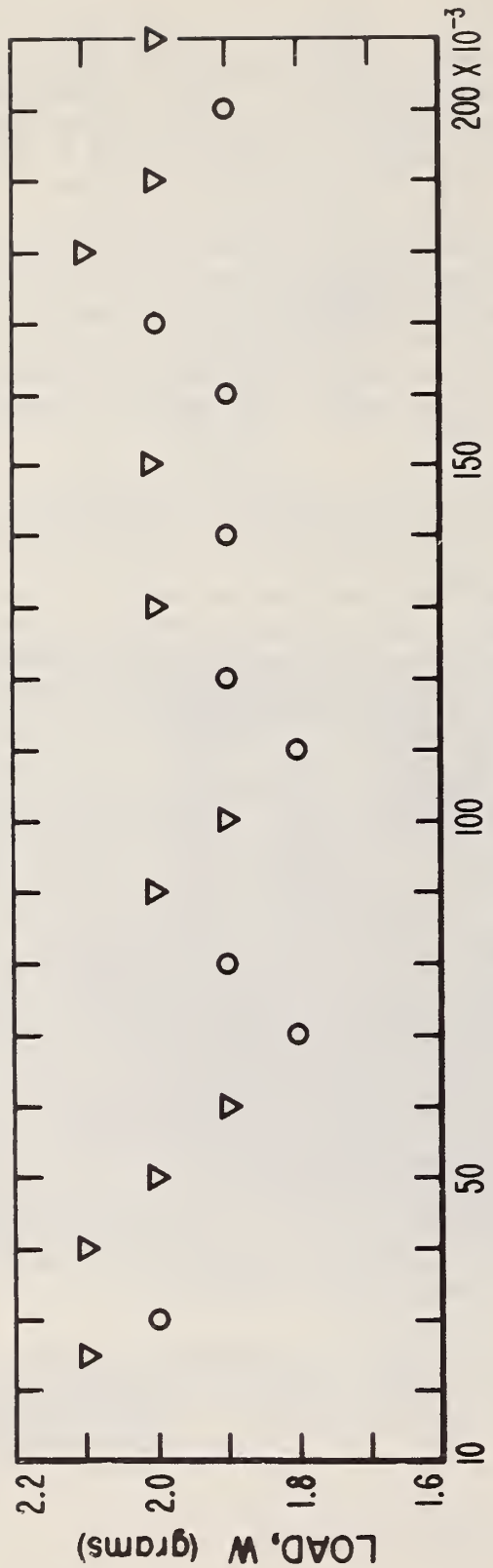

Fig. 6 Test data for the determination of threshold adhesion failure obtained from a set of typical scratch test measurements. Loads at which failure was observed are indicated by ∇; loads at which failure was not observed are indicated by o.

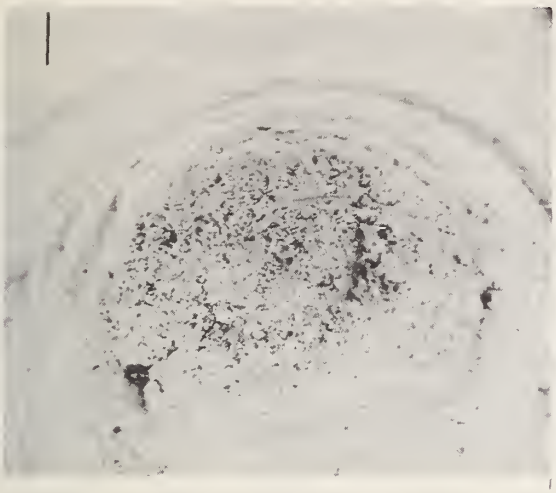

a: Tip of a typical tungsten carbide stylus with a nominal radius of 50 μm before use.

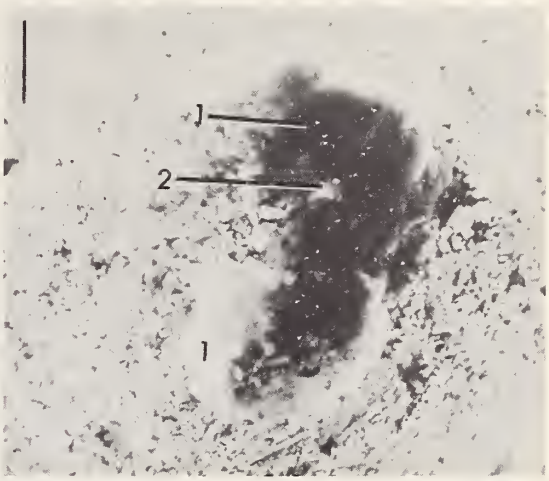

b: Tip of a tungsten carbide stylus with a nominal radius of 50 μm which was used for scratching an aluminum film. Note the agglutination of aluminum at the tip (1) and the single tungsten carbide granule (2) showing through.

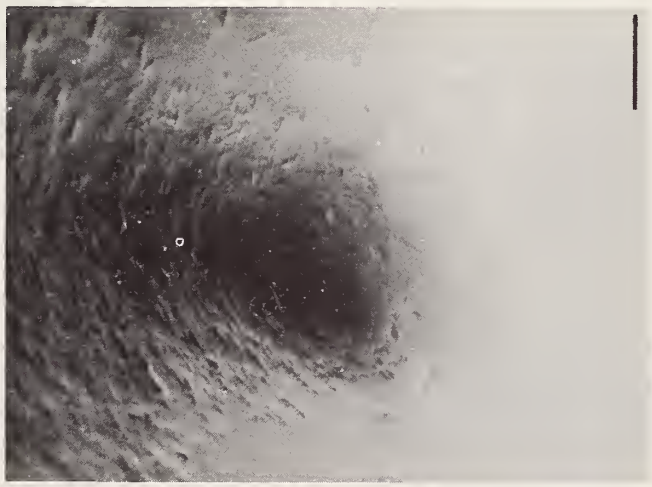

c: The tip of a good commercial diamond stylus with a nominal radius of 20 μm. Notice the exceptional smoothness of this stylus as compared to tungsten carbide.

Fig. 7 SEM photomicrophotographs of stylus tips. In each case the black line represents a distance of 10 μm.

magnification somewhat in excess of 100 X. A reticle-type comparator is then used to match semicircles of known radius to the photograph of the tip profile. Matching can be done within 0.5 mm so that with 130 X magnification a determination of the nominal tip radius within approximately ±4 μm is obtained.

More detailed information about the surface features of the tip of the stylus, which does the actual scratching, can be obtained with the scanning electron microscope (SEM). The tip of a tungsten carbide stylus is shown in Fig. 7a. With higher magnification, the individual grains of tungsten carbide are clearly evident, the smaller ones being about 0.6 μm in size. The tip of the stylus actually used in these experiments is shown in Fig. 7b. Aluminum from the scratched films can be seen on the surface of the tip area. From this photograph it also appears probable that a single granule was responsible for all the cutting. Further enlargements of this area show that the two clearly exposed edges of this granule are about 1.2 μm long and the radius of the included tip is about 0.18 μm. Relative to a metal film thickness of 0.5 μm, this granule represents a fairly sharp cutting edge. The tip of a commercial diamond stylus with a nominal radius of 20 μm is shown in Fig. 7c. From this it can be seen that diamond styli considerably smoother than tungsten carbide styli can be obtained. (J. Oroshnik and W. K. Croll)

Plans: In order to make a comparative behavior study, additional adhesion measurements by the scratch method will be made on the same aluminum-silica system. Measurements will be made with at least one more tungsten carbide stylus and two diamond styli, all having the same nominal 50 μm tip radius of curvature. The measurement precision of the two stylus materials will then be compared; if statistically significant differences are noted the better material will be selected for further testing.

The interferometric method for determining the radius of curvature of this tip will be studied further. The literature search on adhesion testing will be continued as planned. Work on the orthogonal pull test will be deferred until the scratch test has been evaluated more fully.

3.2 PROCESSING FACILITY

Objective: To establish a microelectronics fabrication laboratory consisting of the facilities necessary for the production of specialized silicon devices for use in research on measurement methods.

Progress: The major effort during the last quarter was expended in the improvement and characterization of the existing processes, with emphasis on the production of sets of photomasks and the improvement of

control of diffusion processes. These operations are two of the most critical operations encountered in semiconductor device production.

To assure consistent results in the production of sets of emulsion photomasks, a set of procedures was written describing each operation in detail. Incorporated in the procedures is a method for obtaining alignment keys or reference marks to facilitate the registration of the various masks of a set. Masks were made for oxide-passivated, n^+-p junction diodes for use in the study of voids in die bonding (see Section 3.3). Various stages in the making of this mask set are shown in Fig. 8. A section from the wafer which includes several of these diodes is shown in Fig. 9. A die bonder [2] was obtained with which these diodes can be eutectically bonded to gold-plated TO-5 headers. Voids incorporated into the surface of the header in a controlled way simulate a defective die-bond.

During the past quarter, difficulty was experienced with the adhesion of the photoresist to the silicon dioxide during etching. This resulted in undercutting of the resist and a severe degradation of the pattern being etched. This was found to be caused by insufficient buffering of the etching solution. The problem was solved by lowering the hydrofluoric acid concentration of the etch, and etched patterns in 1-μm thick oxides with no undercutting visible at 400 X magnification can now be obtained.

Diffusion schedules [1] were adopted for both p- and n-type furnaces. The operating procedures which had been used previously yielded diffused wafers with sheet resistances only marginally reproducible (approximately ±20 percent at 20 Ω/square for p-type diffusions and ±10 percent at 7 Ω/square for n-type diffusions – both junction depths were 2 μm in 1 Ω-cm silicon of the opposite type). The flow rates for dopant gas mixtures in the p- and n-type diffusion furnaces were increased from 1600 cm^3/min to 4500 cm^3/min and 3500 cm^3/min respectively. Increasing the flow has improved both the uniformity of the doped oxide and the reproducibility of the sheet resistance. In addition, better thermal transient characteristics of the furnaces were obtained. The compositions of the doping mixtures presently used are listed in Table 1. The p-type furnace is operated at 1050 ± 1°C; the n-type furnace, at 1100 ± 1°C. (T. F. Leedy and J. Krawczyk)

Work was begun on obtaining an operational SCEPTRE computer program at NBS. SCEPTRE [3] provides the circuit analyst with a tool for computing the transient responses of electrical networks. The program is capable of performing d-c steady state and transient analysis. Transient analysis may be performed with initial conditions either specified by the user or calculated from a previous part of the computation.

(T. F. Leedy)

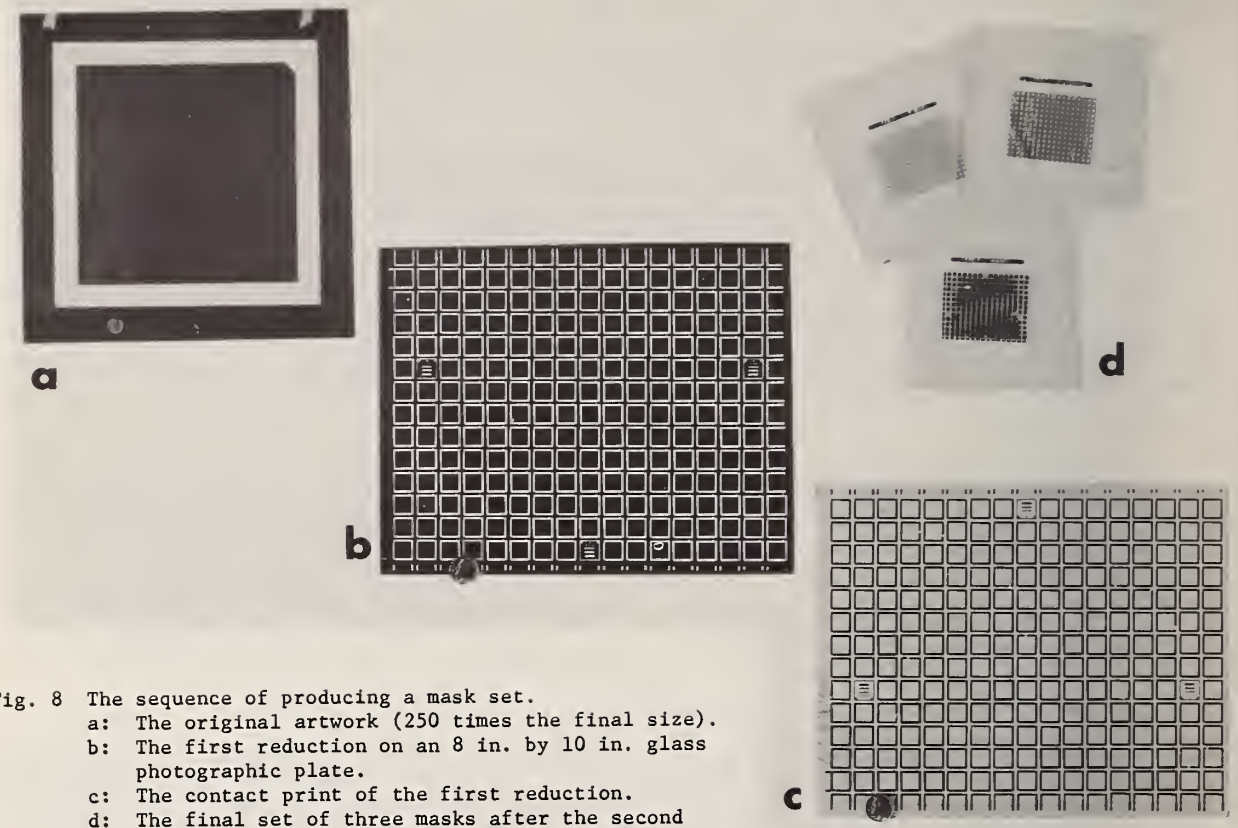

Fig. 8 The sequence of producing a mask set.
a: The original artwork (250 times the final size).
b: The first reduction on an 8 in. by 10 in. glass photographic plate.
c: The contact print of the first reduction.
d: The final set of three masks after the second reduction.

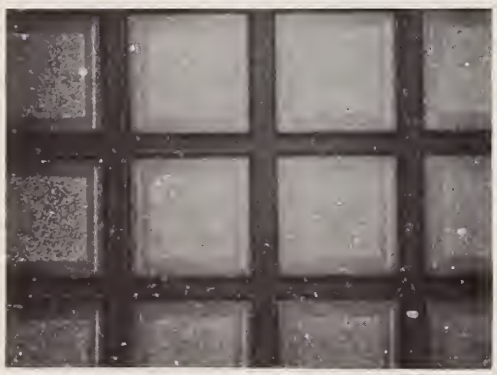

Fig. 9 A section of the diode array produced by the mask set. Final die size is 0.050 in. by 0.050 in.

Table 1. Doping mixture flow rates

Gas	Flow rate	
	p-type	*n*-type
	cm^3/min	cm^3/min
Nitrogen	4330	3265
Oxygen	150	35
Diborane[a]	18	
Phosphine[a]		200

[a] 1-percent mixture of dopant in nitrogen or argon.

Plans: The die bonding machine will be put into operation and procedures for attaching dice to headers will be established. Preliminary investigations of methods for incorporating voids under dice will start.

A test structure will be developed to evaluate further the currently used processing techniques. This structure will include three diffused resistors, a diode, and a transistor. The objective of such a structure is to determine the compatability of the photomasking and diffusion processes and to provide active devices for electrical measurements.

3.3 DIE ATTACHMENT EVALUATION

Objective: To evaluate methods of detecting poor die attachment in semiconductor devices with initial emphasis on the determination of the applicability of thermal measurements to this problem.

Progress: Thermal resistance measurements are presently used to evaluate the quality of the semiconductor device die attachment with varying degrees of success. Present practices for measuring thermal resistance, R_θ, frequently yield results of questionable accuracy and poor reproducibility. Furthermore, when the thermal resistance of the chip-to-header bonding area is small compared to the overall thermal resistance of the device, it may be possible to detect only large voids by means of the thermal resistance technique. The transient thermal response of devices is expected to be more sensitive to voids than the R_θ measurement. For this reason, it was decided to measure transient thermal response in addition to R_θ in the study of diodes with controlled voids.

The processing of diode chips to be used in the void detection studies was continued (see Section 3.2). Further radiographic studies were conducted to establish procedures and techniques for taking X rays of semiconductor devices. (F. F. Oettinger)

Plans: The processing of the diode chips to be used in the void detection studies will be completed. The design and fabrication of equipment which will be used to measure thermal resistance and transient thermal response of the diodes with controlled voids will be initiated.

3.4 WIRE BOND EVALUATION

Objective: To survey and evaluate methods for characterizing wire bond systems in semiconductor devices and where necessary to improve existing methods or develop new methods in order to detect more reliably those bonds which eventually will fail.

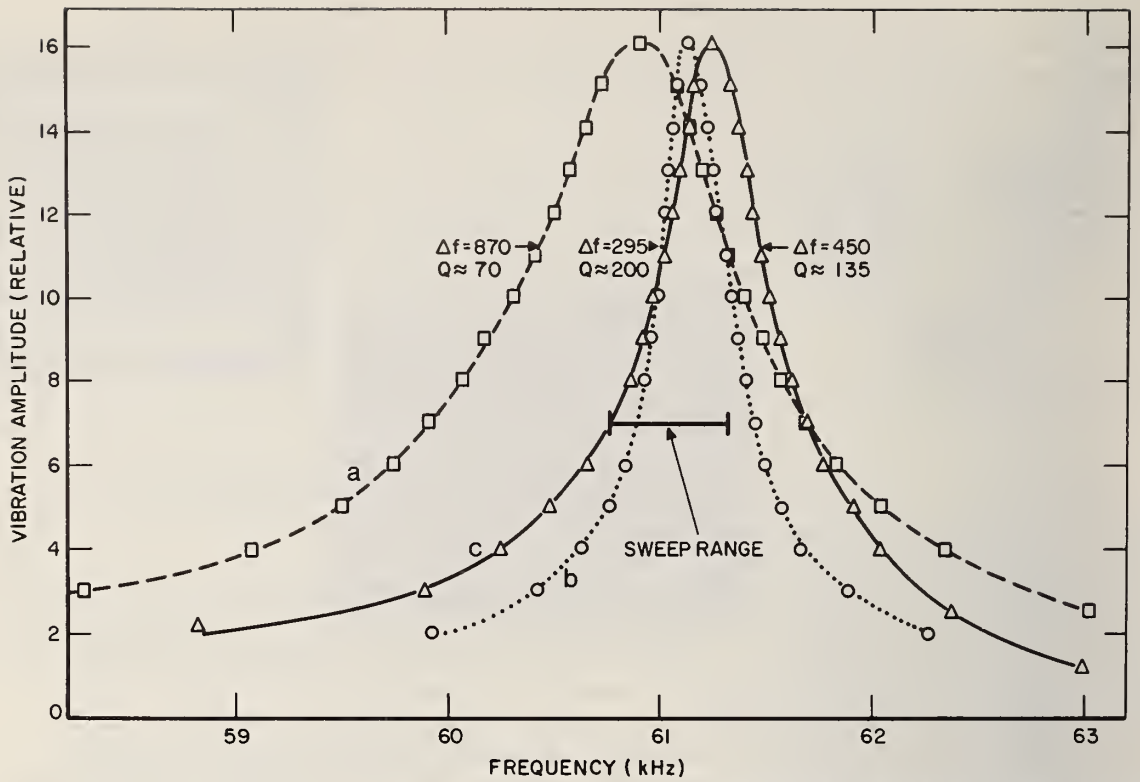

Fig. 10 Mechanical resonance curves taken on the same transducer driven by three different ultrasonic power supplies. In each case the tool extension is 0.555 in.
a: Constant current source.
b: Constant voltage source.
c: Constant power source. (The sweep range indicated is that provided with this supply, see Fig. 13d.)

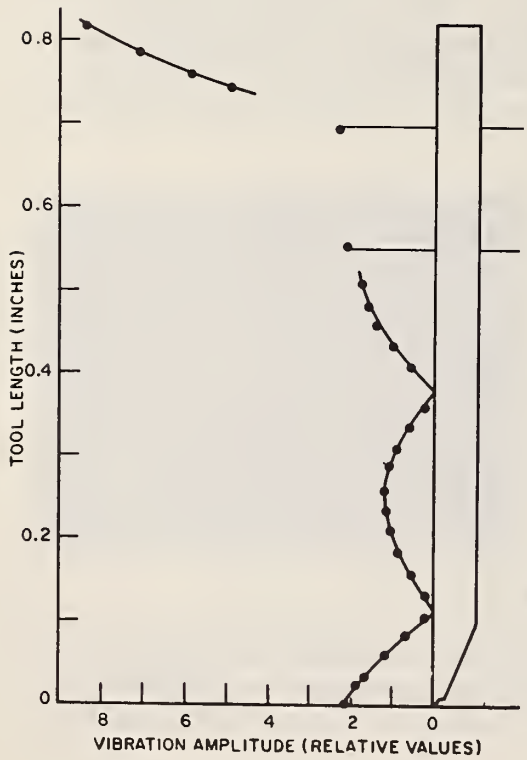

Fig. 11 Vibration amplitude of an ultrasonic bonding tool. The tool extension is 0.555 in. below the horn. The tool extension above the horn is close to a half wavelength and thus the vibration amplitude is much larger than that of the bottom portion of the tool.

Progress: To make wire bonds with reproducible pull strengths, in part for the development of a meaningful method for bond evaluation, the characterization of ultrasonic wire bonding systems used for attaching leads to integrated circuits has continued. The techniques for using a capacitor microphone to study the parameters which affect the motion of bonding tool tips have been improved, and procedures for fabricating bonding pads on both oxidized and unoxidized silicon wafers have been developed. Direct assistance has been given one of the sponsors of the Joint Program. Detailed investigations of wire bonds with the scanning electron microscope has led to the identification of problems associated with the bonding machine used on operational production lines and provided information concerning the pattern of bond formation. An apparatus to evaluate the uniformity of deformation of bonding wire after indentation has been designed. Work on the bibliography and critical review survey paper is continuing.

Characterization of Ultrasonic Bonding Systems — Previous work has shown that slight changes in the power supply impedance can have a significant effect on the mechanical Q of the wire bond system (NBS Tech. Note 495, pp. 26-28). These measurements were made with special laboratory amplifiers in which the current and voltage were individually controlled. Similar measurements have since been made with three commercially available ultrasonic wire bonding power supplies which were used to drive the same transducer-tool combination. The vibration amplitude was measured with a capacitor microphone positioned near the tip of the bonding tool. Mechanical resonance curves obtained with these three power supplies are shown in Fig. 10. As would be expected from the earlier results, it was found that the mechanical Q of the system was lowest when driven with a constant current source (curve a), intermediate when driven with a constant power source (curve c), and highest when driven with a constant voltage source (curve b). For these tests, a 0.828-in. long bonding tool was used with an extension which is commonly used on some bonders, 0.555 in. below the horn.

Investigation of the vibration amplitude along the entire tool length has shown that the tool extension above the horn can significantly affect the resonant frequency and other characteristics of the transducer-tool system. The data shown in Fig. 11 were taken from the same tool driven under the same conditions as were used to obtain the data for curve c of Fig. 10. In this case the residual extension above the top of the horn is approximately a resonant length. Under similar conditions, different bonding tools have been observed to have amplitude maxima above the horn greater than ten times those below the horn. Since the normal tool tolerance is ±0.015 in. and since only the tool extension below the horn is measured when mounting a new tool, it is possible that the residual extension above the horn can vary as much as 0.03 in. from tool to tool. When the measurement was repeated with a different tool, 0.013 in. longer than the one used in the measurement shown in Fig. 11, the

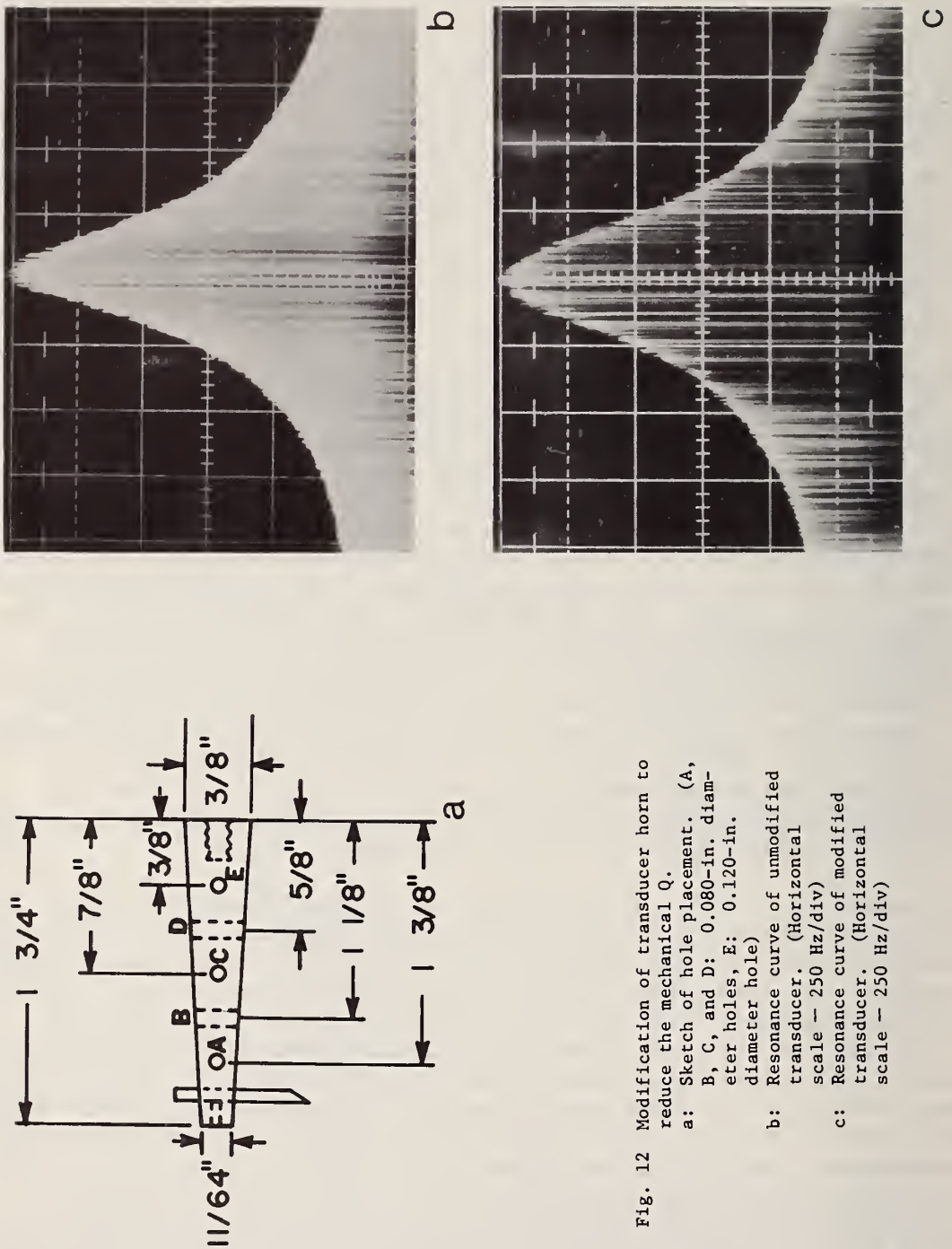

Fig. 12 Modification of transducer horn to reduce the mechanical Q.
a: Sketch of hole placement. (A, B, C, and D: 0.080-in. diameter holes, E: 0.120-in. diameter hole)
b: Resonance curve of unmodified transducer. (Horizontal scale — 250 Hz/div)
c: Resonance curve of modified transducer. (Horizontal scale — 250 Hz/div)

amplitude of the top portion was similar to that of the bottom. The changes in system resonant frequency and mechanical Q which result from large resonances of the top of the tool require significant adjustment of the ultrasonic power supply power control setting to reestablish the original bonding tool motion. It was also observed that, when the maxima above the horn were as much as ten times those below, these parameters become critically dependent on the tightening torque applied to the bonding tool set screw.

Since mechanical resonance curves measured with a capacitor microphone have been very useful in characterizing ultrasonic wire bonders, a simple system of generating them was constructed. A small, variable capacitor with a linear potentiometer attached to its shaft is connected across the oscillator coil of the ultrasonic power supply. The potentiometer is used to control the voltage which is applied to the horizontal input of an oscilloscope. When the capacitor is manually tuned, a complete resonance curve is generated, picked up by the microphone, and displayed on the oscilloscope. Such a system permits the rapid comparison of resonant curves taken under different conditions.

In order to lower its mechanical Q a series of holes was drilled in the horn of an older transducer as shown in Fig. 12a. The resonance curve with the unmodified transducer obtained with the above system is shown in Fig. 12b. The initial Q of this particular transducer-tool-power supply combination was 165. After the modification, the Q dropped to 125 as shown in Fig. 12c, a decrease of approximately 25 percent. The mechanical resonance frequency decreased only 2.6 kHz. For both measurements the same bonding tool and power supply were used and the bonding tool extension and power supply settings were reproduced as accurately as possible. Thus it can be seen that by means of a simple modification the mechanical Q of an existing transducer can be lowered significantly while the frequency and amplitude remain essentially unchanged. The broader resonance peak obtained in this way reduces the detuning effects of thermal environmental changes and instabilities in the oscillator.

Frequency modulation of the power supply oscillator is another technique which is often used to reduce the problems associated with thermal and oscillator instabilities. The characteristic motion of the tool tip which results from frequency modulation of the 60-kHz power supply oscillator of a bonding machine transducer was studied in some detail by means of the capacitor microphone. The response of the tool tip vibration amplitude to a square-wave modulation voltage is shown in Fig. 13a. The rise time (10 to 90 percent) was 1 ms whereas the rise time of the modulating pulse was much shorter. The mechanical Q calculated from the time required for the amplitude to decay to one half its equilibrium value agrees very well with the measured static Q of the system (curve c, Fig. 10).

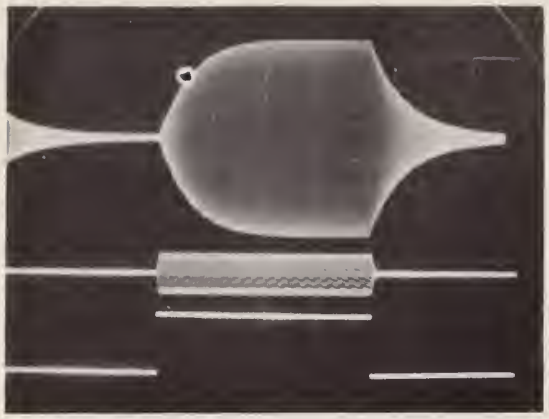

a: Square-wave modulation.

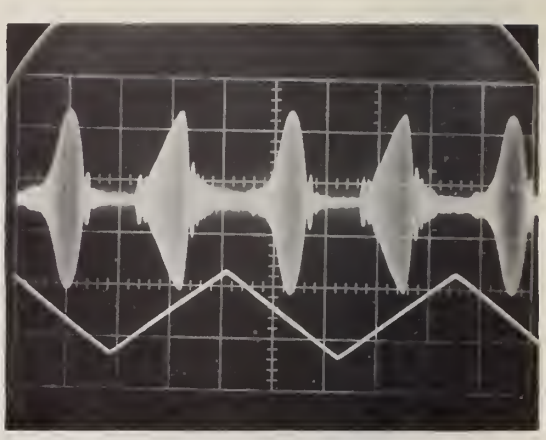

b: Triangular-wave modulation.

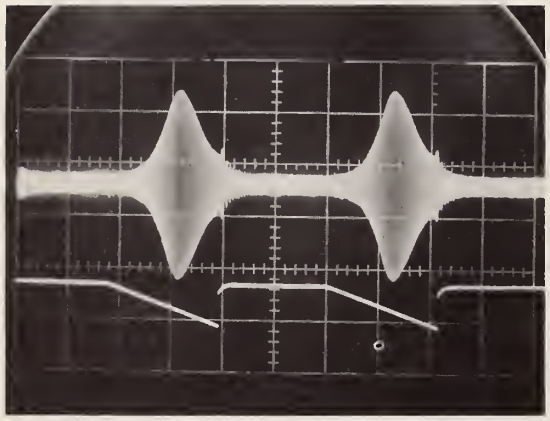

c: Saw-tooth modulation (decreasing frequency).

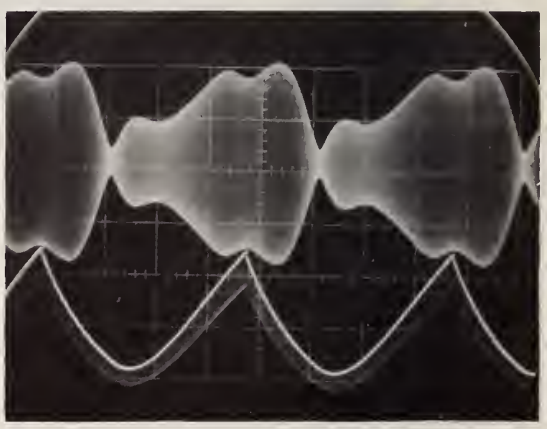

d: Modulation wave-form supplied with power supply.

Top curve: Vibration amplitude of the tool tip as measured with a capacitor microphone.
(Vertical scale — 0.5 mV/div)
Bottom curve: Modulation voltage applied to oscillator.
(Vertical scale — a: 0.5 V/div;
b, c: 1 V/div;
d: 0.1 V/div)
Center curve (a only): Power supply oscillator output voltage.
(Vertical scale — 2 V/div)

(Horizontal scale — a, d: 1 ms/div;
b, c: 5 ms/div)

Fig. 13 Response of the bonding tool vibration amplitude to frequency modulation of the power supply oscillator

A linear frequency drive was introduced into the power supply oscillator by means of a triangular-wave modulation voltage with the result shown in Fig. 13b. The frequency changed linearly with voltage, but the vibration amplitude envelopes for increasing and decreasing frequency were not the same. The decreasing frequency envelope resembled a normal resonance curve; however, the increasing frequency envelope was compressed toward the high frequency end. This effect is presumed to result from the slow mechanical rise time of the system. In the increasing frequency case, not only the tool tip amplitude but also the frequency is increasing. Thus the net acceleration of the motion is significantly higher, equivalent to frequency modulation at a considerably higher sweep rate. Conversely, by sweeping toward lower frequencies, a lower mechanical acceleration is applied to the system, and a more nearly quasi-static sweep results.

If the slow mechanical response of the system is taken into account, it is possible, by adjusting the sweep rate, amplitude, and center frequency and by using a saw-tooth modulation voltage, to obtain a symmetrical system response curve that is closely related to the static resonance curve c of Fig. 10. The result shown in Fig. 13c was obtained on the same transducer-tool system with the same tool extension and the same power supply as were used to obtain the static resonance curve.

Studies of the frequency modulation in some commercial power supplies have revealed that the frequency may not always be swept through the entire static resonance peak. In a typical case the sweep starts from the lower frequency side, barely goes over the resonance peak, and then returns toward lower frequencies. The result shown in Fig. 13d was obtained when the transducer system was tuned by the method recommended by the manufacturer. The sweep range for this case is shown in Fig. 10. A possible result of such a partial sweep technique is that the resonance frequency detuning due to the temperature sensitivity of the transducer may be effectively increased if the resonance peak shifts in such a way that the modulating voltage is not large enough to reach the new maximum.

Extensive assistance was given one of the sponsors in connection with with wire bonding problems encountered on production lines. A detailed procedure for trouble shooting and tuning bonding machines and determining their mechanical stability with the capacitor microphone is being prepared for issuance as a NBS Technical Note. Several potential problem areas in addition to those discussed above were also identified. Many marks and scratches were found on the anodized aluminum spools that are used for holding the 0.001-in. aluminum bonding wire. In some instances clear impressions left by the wire on the spool as depicted in Fig. 14 were observed. It is possible that some of the spool material can stick to the wire and be carried along the wire feed path or onto the semiconductor die. In an investigation of possible contamination along the wire feed path, a large accumulation of white particles was observed in

Fig. 14 Wire marks (2) in the coating of a spool left by 0.001-in. diameter aluminum bonding wire. Other marks shown (1) are tooling marks. Magnification: 60 X.

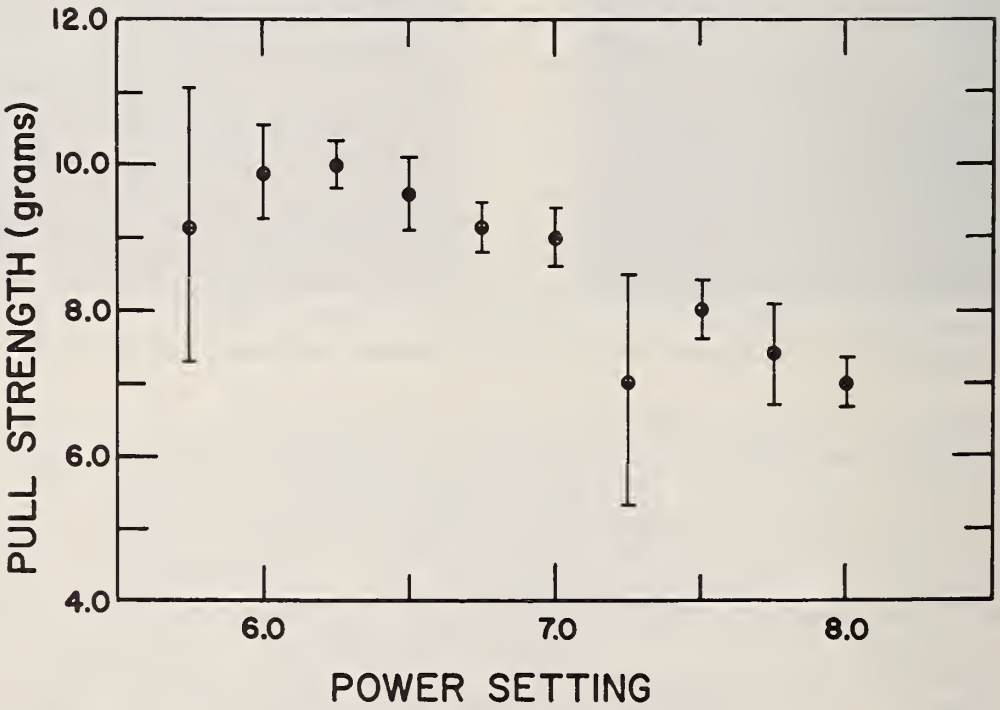

Fig. 15 Pull strength in grams as a function of bonder power setting for oxidized substrate, aluminum sintered at 550°C. Intervals shown are 95 percent confidence levels for the mean.

a relatively new transducer wire feed hole through which less than two spools of wire had been passed.

The mechanical stability of the bonding machine was checked by means of a capacitor microphone and a laser beam reflected from a mirror on the cam housing onto a distant wall. Relatively low frequency mechanical vibrations were observed between the top portion of the machine that houses the transducer cam and motor and the base that clamps the semiconductor die. This motion was attributed to the cantilever type of support provided for the transducer housing. The motion was very noticeable when the cam motor was turning. This vibration may cause the displacement of wire during bonding which has been observed in some cases with the scanning electron microscope (see Fig. 17d, p. 43).

Temperature characteristics of an ultrasonic transducer system were measured last quarter (NBS Tech. 520, pp. 40-41). One commercially available bonding machine used in this study is supplied with a large-area, high-intensity lighting system which is capable of heating the general bonding area between 5 and 10°C above the ambient temperature. As the entire unit warms up, the resonant frequency drifts downward 100 to 200 Hz. To obtain reproducible bonding conditions with this machine, it was necessary to preheat the transducer by turning the lights on for several hours prior to bonding or to put a heat absorbing filter in front of the lamps.

The fixture used on this machine to hold the transistor or integrated circuit is designed to be rotated manually; the operator's hand normally contacts it during the bonding operation. Measurements made with the capacitor microphone revealed that slight motion of the hand could move the fixture as much as 0.001 in. Such motion of the fixture can cause undesirable skidding of the wire across the pad during bonding.

(G. G. Harman and H. K. Kessler)

An improvement in the taper tip used to increase the resolution of the capacitor microphone (NBS Tech. Note 520, pp. 63-66) was achieved with the fabrication of precision, stainless-steel taper tips. The performance of these tips is similar to ones made of aluminum foil; however the steel tips are considerably more rugged and therefore more practical for frequent tuning of bonding machines as might be required on a production line. (L. M. Smith)

Fabrication of Bonding Pads — The bonding pads that were used for the work reported here are fabricated on 0.01-in. thick, 1-in. diameter silicon wafers, coated with 0.5 μm of steam-grown silicon dioxide and 0.5 to 1 μm of evaporated aluminum. The aluminum is etched to leave 0.005-in. square bonding pads by means of standard photolithographic techniques. The photomasks for these patterns were made from readily available Ronche rulings which can be obtained from optical suppliers. When two-level

a: Normal configuration.

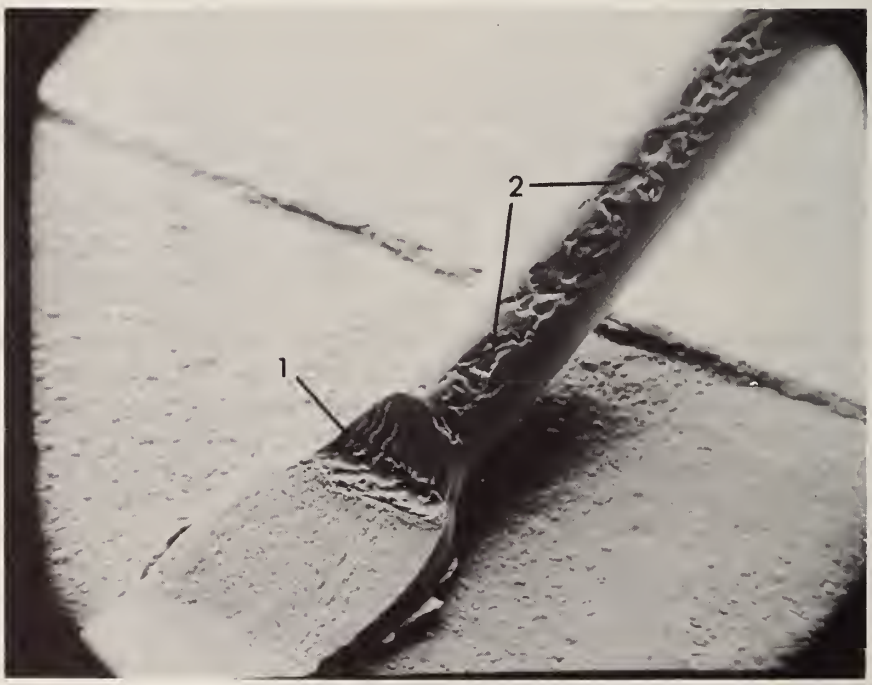

b: Wire has twisted after being clamped and before bonding.

Fig. 16 SEM photomicrographs (575 X) of aluminum ultrasonic wire bonds showing heel crack (1) and clamp marks (2). The clamp marks appear on both sides of the wire.

bonding is desired, strips are cut from similar wafers and epoxied to multi-level substrates. Finally the entire wafer is bonded with epoxy to a steel holder so that hundreds of bonds can be made without changing wafer or other bonding conditions.

This procedure was selected as a result of an evaluation which was made of substrates prepared with different sintering temperatures in order to establish conditions which yielded reproducible bond strengths as determined by a pull test. Silicon wafers were prepared in pairs. One wafer of each pair had a 0.75-μm thick layer of thermally-grown oxide while the other did not. A 0.5-μm thick aluminum film was evaporated on each wafer. After the array of square bonding pads was etched, pairs were sintered for 15 min at 425, 500, 550, and 577°C in a helium atmosphere.

Ultrasonic bonds were made on each specimen with 0.001-in. diameter aluminum wire at various power settings of the ultrasonic wire bonder. The single-loop wire bond strength was measured by a pull test with a simple hook at the center of the loop. By means of a one-sided t-test at a 95 percent confidence level [1], it was found that the oxidized specimens sintered at 500 and 550°C were statistically similar and that they both yielded higher pull strength than the oxidized specimens sintered at either 425 or 577°C. As an example, the curve for the 550°C specimen is shown in Fig. 15. The two-sided 95 percent confidence level for the mean is indicated for each point plotted. For the unoxidized specimens, the curves were uneven and the results were inconclusive.

(K. O. Leedy, J. K. Madello, and J. Krawczyk)

Scanning Electron Microscopy — Bonds from several devices selected from the output of operational production lines were examined with the scanning electron microscope (SEM). The bonding machine used on these lines has a tool motion such that the vibrating tool is inclined forward 4 deg from the normal for the first bond and is perpendicular to the die surface for the second bond. The crack in the wire at the heel of the bond as shown in Fig. 16 is a feature of all first bonds made by this machine. In addition, deep indentations, also shown in Fig. 16, were observed on the sides of the wire. It has been determined by additional SEM photographs that these marks are produced by the jaws of the clamping system through which the wire is fed from the spool to the bonding tool. In addition to marring the surface finish, these imprints could work-harden the wire and thus affect bonding conditions. Occasionally the wire twists after passing through the clamping system, and the indented portion then becomes a part of the actual bond interface as shown in Fig. 16b. Of particular concern is the possibility of contamination from the clamp becoming embedded in the wire and directly interfering with the bonding process. Since the twists, such as those depicted in Fig. 16b, occur only occasionally and since not all of these need be significantly contaminated, the possibility should be considered that this may be a cause of occasional, otherwise unexplained weak bonds.

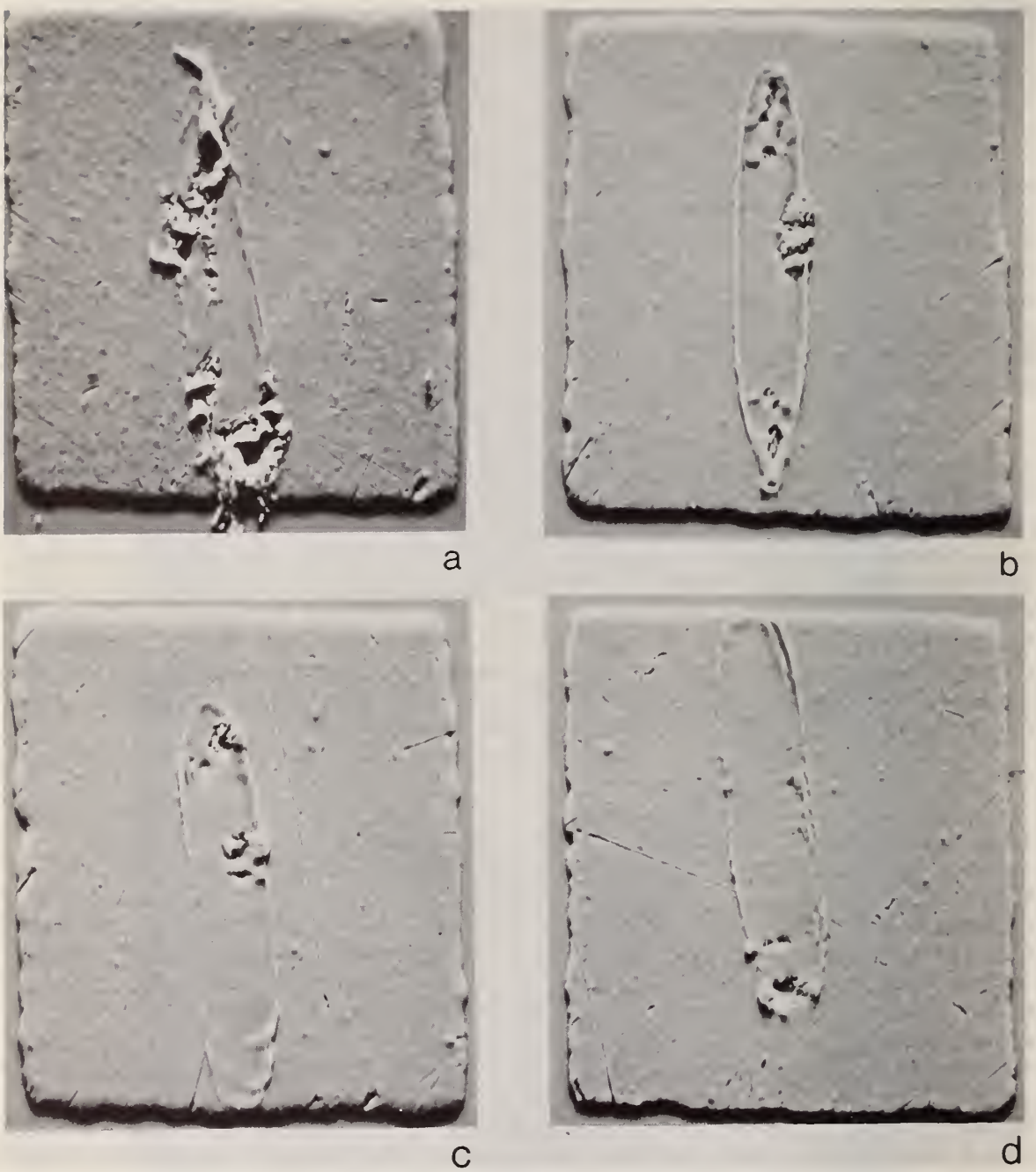

Fig. 17 SEM photomicrographs (460 X) of bond adhesion (lift-off) patterns for first bonds made at different time settings and constant power setting. The time is longest for case a and is decreased to the shortest value for case d. Settings used in case a result in a bond which will adhere to the pad; the shorter time settings do not produce an adherent bond. Note that the scratches on the bonding pads (which result from a cleaning process no longer in use) are polished out by the ultrasonic motion of the compressed wire even before appreciable bonding occurs. Note also the apparent movement during bonding exhibited in case d. This is thought to result from mechanical vibration in the bonding machine.

By studying the bonding pad after a bond has been intentionally lifted or peeled off, the pattern of bond formation can be seen. The threshold of welding can be observed by decreasing either the power or time in the bonding schedule to a point where essentially no bonding has taken place. This experiment was performed for a number of first and second bonds. An example is shown in Fig. 17.

In all cases, bonding begins at localized points and then, as the power or time is increased, the weld extends to other areas, usually the toe or the heel or both. The next areas to weld are the sides; the center is the last portion to weld. Even in some very strong bonds, the center area generally remains unbonded. This is illustrated in Fig. 18 which shows the pad under a strong bond which has been peeled off with a force of 8 g.

Although there are general characteristics of bond patterns which can be observed, it is premature to draw firm conclusions about the bonding process from these initial studies. However certain facts are evident. From cases in which very low power or short time was used, such as that shown in Fig. 17d, it appears that most of the deformation of the wire occurs before welding begins. The unwelded area under the wire becomes polished as a result of the ultrasonic motion of the compressed wire. When welding begins, it starts at tiny, isolated points which are seldom located in the same positions for successive bonds. Occasionally the weld will start in entirely different sections of the bond. An example of two consecutive first bonds made with the same bonding conditions is shown in Fig. 19. One possible explanation for these observations is that the hard silicon precipitates in the 1-percent-silicon doped wire are necessary, or at least help, to start the substrate abrasion which leads to welding. This suggests the need for further studies in which the lifted off wire is observed with an electron microprobe in order to determine the presence or absence of silicon precipitates at the initiating points.

Another problem which is apparent in the lift-off patterns is that of bonding machine movement during the bonding which was discussed earlier. An example of such movement can be seen in Fig. 17d.

Wire Evaluation — Additional evaluation of ribbon wire has been delayed because it has not been possible to obtain ribbon wire of higher tensile strength in the desired size. (K. O. Leedy)

A wire tester has been designed for determining the uniformity of the deformation of aluminum bonding wire. The wire is indented automatically at regular intervals and the extent of the deformation is detected by a displacement sensor. The results of this test are affected by variations in both diameter and hardness of the wire. Measurements of the uniformity of deformation are expected to be of value in the

Fig. 18 SEM photomicrograph (800 X) of bond adhesion (lift-off) pattern for a strong first bond.

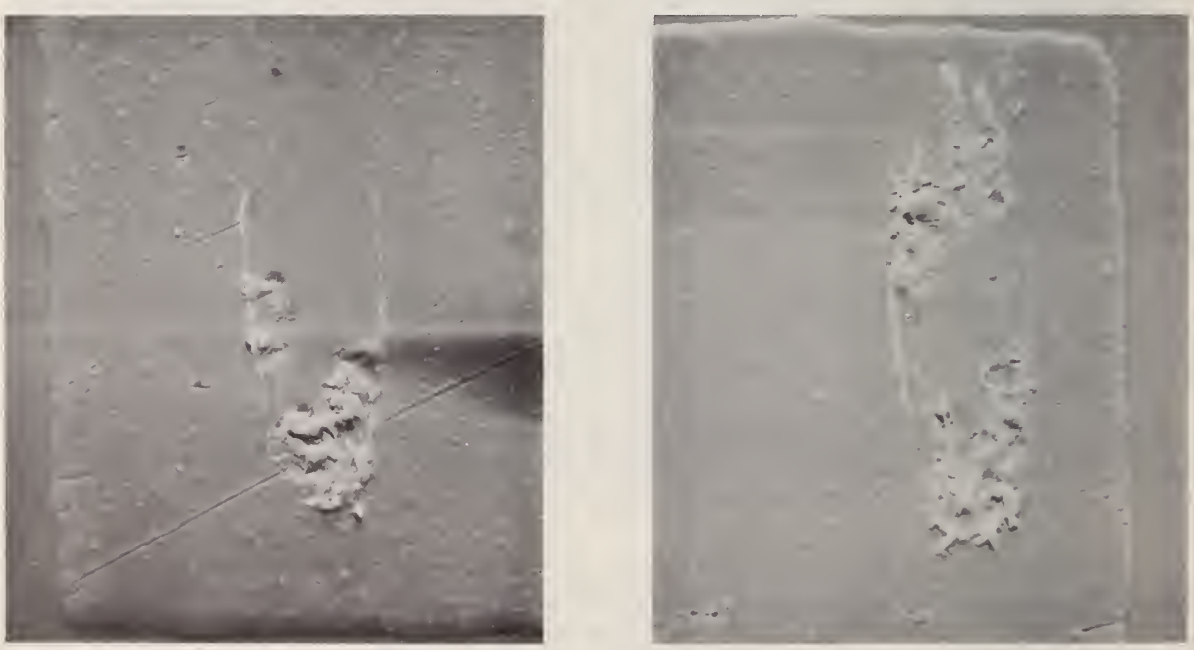

Fig. 19 SEM photomicrographs (600 X) of bond adhesion (lift-off) patterns for two second bonds made consecutively at identical time and power settings.

selection of wire to be used in the evaluation of the pull test and other tests for wire bond quality.

Pull Test Evaluation — A low-duty cycle, high-current pulser and probe system, originally designed and constructed to evaluate the high-current pulse method for testing bond quality has been adapted for the purpose of cutting the loop between two bonds without otherwise damaging the bonds. Since normal bonding machines make two bonds with a loop between, it is necessary to cut the loop without pulling or damaging either the wires or the bonds in order to test each bond separately. Then the hot-melt glue bond puller (NBS Tech. Note 488, pp. 22-24) can be used to determine the individual bond strengths. The new technique for cutting the loop represents an improvement over previously used, mechanical procedures. (H. K. Kessler)

Bibliography and Critical Review — The collection of papers for the bibliography is essentially complete. Although earlier work has been obtained either from reference citations or from the bibliographic search prepared by the Defense Documentation Center (DDC), which included reports published as early as 1953, major emphasis has been given to the collection of papers and reports which have appeared in the period 1965 to 1969, inclusive. Each issue of about 30 journals published during this period was scanned. Because the report file from which the DDC search was prepared does not contain all NASA documents, issues of *Scientific and Technical Aerospace Reports* published during this period were also scanned. More than 80 articles and reports that are considered significant have been assigned key words for their inclusion in the bibliography. (H. A. Schafft and E. C. Cohen)

The first draft of the introduction and much of the section on the evaluation of wire bond systems has been written for the critical review survey paper.

In general, the evaluation methods that have been found in this survey are used to perform one or more of the following three functions: to optimize bonding procedures, to determine if the bonding procedures remain controlled, and to determine the quality of the wire bond system. Detailed analyses of three commonly used methods (visual inspection, double bond pull tests, and centrifuge tests) were undertaken.
(H. A. Schafft)

Plans: Evaluation of ultrasonic bonding machines will continue. This will include further consideration of problems encountered on production lines. A simple milliwatt laser interferometer will be constructed for use in conjunction with the capacitor microphone to study tool and transducer motion during the bonding process.

Experiments for the purpose of evaluating the importance of variable parameters of the bonder, such as power and bonding time, with respect to the pull test will be designed. A bonding tool design most appropriate for making bonds for these experiments will be selected. Work on the modification to the bond puller will resume. The modified puller will also have the capability of varying the pull rate and of prestressing bonds to a fixed-force level in addition to providing a means of recording the force at which the bond failed.

The scanning electron microscope will be used for studying bonding wire. Sections of bonding wire with which good bonds could not be made will be studied in an effort to evaluate the effect of inhomogeneities in the wire which might be responsible for its poor performance. Study of lift-off patterns will continue.

Work on ribbon bonding wire will resume. The wire testing machine will be assembled and tested.

The first draft of the critical review survey paper and the assignment of key words to all the papers to be included in the bibliography will be completed.

3.5 REFERENCES

3.1 Metallization Evaluation

1. M. M. Karnowsky and W. B. Estill, "Scratch Test for Measuring Adherence of Thin Films to Oxide Substrates," *Rev. Sci. Instrum.* 35, 1324-1326 (1964). A standard method based on similar principles is being developed by ASTM Committee F-1.

2. O. S. Heavens, "Some Factors Influencing the Adhesion of Films Produced by Vacuum Evaporation," *J. Phys. Rad.* 11, 355-360 (1950).

3. P. Benjamin and C. Weaver, "Measurement of Adhesion of Thin Films," *Proc. Roy. Soc. (London)* 254-A, 163-176 (1960).

4. L. E. Collins, J. G. Perkins, and P. T. Stroud, "Effect of Ion Bombardment on the Adhesion of Aluminum Films on Glass," *Thin Solid Films* 4, No. 1, 41-45 (1969).

5. M. L. Hair and A. M. Filbert, "Surface Chemistry of Glass," *Research/Development* 20, No. 10, 34-38 (1969).

6. M. G. Natrella, *Experimental Statistics*, NBS Handbook 91, August 1, 1963, pp. 10-22 to 10-23.

3.2 Processing Facility

1. R. M. McLouski, "Diffusion of Impurities into Silicon from Gaseous Sources," NASA CR-524 (November, 1966). (Available from the Clearinghouse for Federal Scientific and Technical Information (CFSTI), Springfield, Va. 22151, N66/39891)

2. R. J. Anstead, "Semiconductor Wafer Bonder," TM-66-4 (April, 1966). (Available from CFSTI, AD 634030)

3. S. R. Sedore, "SCEPTRE: A Program for Automatic Network Analysis," *IBM Journal* 11, 627-637 (1967).

3.4 Wire Bond Evaluation

1. M. G. Natrella, *Experimental Statistics*, NBS Handbook 91, August 1, 1963, p. 3-34. The NBS Omnitab Computer Program was used in the statistical evaluation for this experiment.

4. METHODS OF MEASUREMENT FOR SEMICONDUCTOR DEVICES

4.1 THERMAL PROPERTIES OF DEVICES

Objective: To evaluate and, if necessary, improve electrical measurement techniques for determining the thermal characteristics of semiconductor devices.

Progress: The literature search and the review of the methods of measurement of thermal resistance and transient thermal response of semiconductor devices were continued. The writing of the first draft of the section of the review paper on steady-state thermal resistance measurements was continued. The identification of key words for the bibliography was initiated. (M. Sigman and F. F. Oettinger)

Last quarter the measurement of d-c current gain, h_{FE}, versus collector-emitter voltage, V_{CE}, was automated. Initial measurements made on a limited number of transistors showed an abrupt decrease in h_{FE} as the device went into a current-constricted operating mode. It was also found that the re-trace of the h_{FE} versus V_{CE} curve did not follow the original trace, but that a hysteresis effect was in evidence (NBS Tech. Note 520, pp. 49-52).

Preliminary measurements of h_{FE} versus V_{CE} were made for several transistors representing a variety of production techniques, geometries, and manufacturers. The devices were interdigitated, planar, triple-diffused or epitaxial-diffused power transistors. Initial results indicated that although a decrease in h_{FE} did occur at the onset of lateral thermal instability it was not always an abrupt change. It was found that the shape of the h_{FE} curve as well as the associated hysteresis effect was dependent on the collector current level as well as on the severity of the current constriction.

Because of the quantity of data required for each device in this study it was decided to determine how best to automate the measurement of thermal resistance, R_θ, versus V_{CE}. The existing equipment has been partially automated for ΔT measurements and plans are underway to determine the feasibility of using a sample-and-hold technique to automate the measurements completely. Then R_θ would be obtained by dividing the transistor power dissipation into the temperature difference between the device junction and the case, ΔT_{J-C}, which is accomplished with an analog divider.

The block diagram of the apparatus now being used to generate and plot ΔT as a function of V_{CE} for constant collector current, I_C, is shown in Fig. 20. The device under test, DUT, is operated in a common-emitter configuration with a variable, current regulated source driving the base. An operational amplifier (I_B SERVO) adjusts I_B to keep I_C

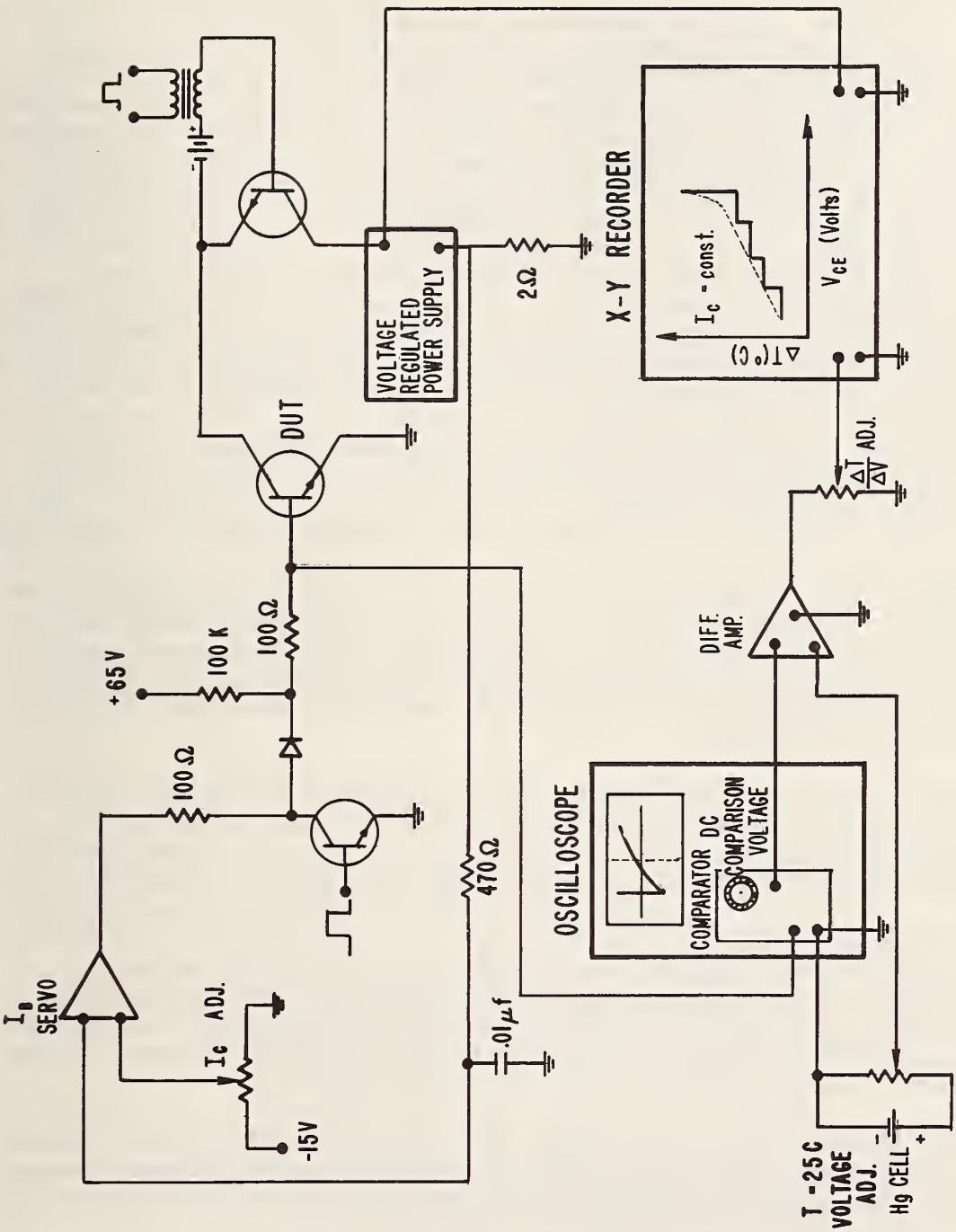

Fig. 20 Block diagram of apparatus used to generate and plot curves of the temperature difference between the device junction and the case as a function of collector-emitter voltage with the collector current held constant.

constant as V_{CE} is varied. Thermal resistance is measured using V_{BE} as the temperature indicator by interrupting the collector voltage supply and simultaneously reducing the base drive to the required low-level metering current. This is accomplished at a repetition rate of from 2 to 20 Hz. The low-level metering portion of the cycle is less than 0.1 percent of the total. An x-y recorder is used to display ΔT_{J-C} as a function of V_{CE}. The d-c comparison voltage of a high gain differential comparator plug-in oscilloscope unit, which is made equal to the forward voltage of the emitter-base junction, V_{BE}, at a specified time after interrupting the collector supply voltage, is subtracted from a reference potential equal to V_{BE} for a junction temperature of 25°C by means of a differential amplifier. The temperature coefficient of V_{BE} is used to convert the output voltage of this differential amplifier to ΔT_{J-C} by means of a suitable voltage divider. The output of this voltage divider is fed into the y-input of the recorder. The plot of ΔT_{J-C} versus V_{CE} is generated by first increasing V_{CE}, which moves the pen of the recorder parallel to the x axis, and then adjusting the d-c comparison voltage to obtain a value of V_{BE} appropriate to the value of V_{CE}. This procedure is continued until the trace is completed. The trace generated is a series of steps from which the curve of ΔT_{J-C} is derived by connecting the end points after each step increase.

(S. Rubin, R. L. Gladhill, and F. F. Oettinger)

Plans: The literature search will continue. The identification of key words for the bibliography will be completed and their assignment to relevant articles initiated. The first draft of the section of the review paper on steady-state thermal resistance measurements will be completed, and work on a second, independent section on transient thermal response will be started.

The merits of fully automating the R_θ measuring system by replacing the manually-operated comparator plug-in unit and oscilloscope by a sample-and-hold unit will be studied. If it is found to be both feasible and warranted, the required circuit modifications will be made.

Consideration will be given to a test circuit similar to the V_{BE} measuring apparatus which will measure R_θ using the collector-base voltage, V_{CE}, as the temperature sensitive parameter. This will allow a study of the reason for the higher measured temperature of the emitter junction over the collector junction [1], even though it is assumed that the power is being dissipated at the collector junction.

Further measurements of R_θ and h_{FE} as a function of V_{CE} will be made on transistors representing a variety of production techniques and geometries and an attempt will be made to correlate the results from the thermographic phosphor study (see Section 4.2).

4.2 THERMOGRAPHIC MEASUREMENTS

Objective: To evaluate the utility of thermographic techniques for detection of hot spots and measurement of temperature distribution in semiconductor devices.

Progress: The photometric equipment was modified to facilitate the study of hot-spot formation and the heat exchanger was improved to permit better control of transistor case temperature. A test fixture for the study of the temperature sensitivity and spatial resolution of the phosphors was fabricated. Studies of the extent and temperature of hot spots as a function of collector-emitter voltage were begun, but data are too limited to draw any conclusions at this time.

Time was spent in becoming familiar with the operation of an infrared microradiometer which was loaned to us by one of the Joint Program sponsors. A device test fixture and heat sink for use with the automatic stage of this instrument was designed and fabricated.

(G. J. Rogers, F. F. Oettinger, and L. R. Williams, Jr.)

Plans: Studies of hot spots and their relationship to the electrically determined thermal characteristics of transistors will be continued. Experiments will also be carried out to determine if coating thickness or the material under the coating has an effect on temperature resolution of the phosphors and to determine the effect of coating thickness on spatial resolution.

The infrared microradiometer will be used to assist in evaluating the relative merits of the phosphor and infrared techniques.

4.3 MICROWAVE DEVICE MEASUREMENTS

Objective: To study the problems and uncertainties associated with measurement of microwave device properties and to improve the methods of measurement for related characteristics.

Progress: Continuing discussions have been held with representatives of the Electronic Industries Association, the Naval Electronic Systems Command, the Naval Applied Science Laboratory, and others to determine the work which is to be undertaken on microwave diode and transistors.

Work was continued on the error analysis for transistor scattering parameter measurements in cooperation with JEDEC Committee JS-9 on Low Power Transistors Task Group on Transistor "S" Parameter Measurements. A survey was made of manufacturers of measurement equipment for microwave transistor "S" parameters to collect existing error analyses of

commercial equipment. Very little data exists on the errors inherent in these instruments at the low signal levels required for linear transistor measurements.

Some of the apparatus which is required for the measurement of mixer diode noise parameters at X band is on hand and has been assembled. The set up can not be completed until more equipment is obtained.

(R. C. Powell and J. M. Kenney)

Plans: Transistor scattering parameter measurement evaluation will continue. Assembly of the mixer diode noise apparatus will continue as equipment becomes available. A survey of mixer diode noise measurement techniques will start.

4.4 SILICON NUCLEAR RADIATION DETECTORS†

Objective: To conduct a program of research, development, and device evaluation in the field of silicon nuclear radiation detectors with emphasis on the improvement of detector technology, and to provide consultation and specialized device fabrication services to the sponsor.

Progress: Silicon detectors obtained for use on earth-oriented satellites and sounding rockets were tested and evaluated with respect to performance specifications and stability. Special lithium-compensated silicon detectors for use in future satellite experiments were fabricated and tested. The performance degradation of surface-barrier detectors by the radiation damage effects of low-energy protons was studied. Assembly of the system for the automated testing of large numbers of detectors has progressed slowly because key parts were not available. Further characterization of large-diameter, dislocation-free silicon for use in lithium-compensated detectors has been deferred for six months because of the heavy work load in other areas requested by the sponsor.

Testing and Evaluation — Totally depleted surface-barrier detectors, with nominal area and thickness of 50 mm^2 and 100 μm, respectively, were extensively tested prior to incorporation into the very low-energy radiation detection system for the IMP-I satellite. The temperature of detectors in the spacecraft is expected to be within the range between -10 and 40°C. The reverse current, noise, and alpha-particle resolution of each detector was measured as a function of applied reverse bias at operating temperatures of -10, 23, and 40°C. Capacitance and bias for

---

† Supported by Goddard Space Flight Center, National Aeronautics and Space Administration. (NBS Project 4254429) Irradiations were carried out at Goddard Space Flight Center.

total depletion were also determined but only at 23°C. In general, the detector current and noise decreased with temperature as expected while there was little change in the alpha particle energy resolution. Operation of surface-barrier detectors at temperatures only a few degrees below room temperature can result in significantly reduced current and noise levels primarily because the thermal generation of carriers decreases exponentially with temperature. Critical requirements for the use of detectors on satellites are that the detector noise remain within acceptable bounds and that bias across the detector always be large enough to insure total depletion of the device over the expected range of operating temperatures.

A series of five special Si(Li) detectors in the form of cubes, 3-mm on a side, were fabricated and tested for use as proton detectors on future TIROS and IMP satellites. The resolution of these devices operating at room temperature and at 300 V reverse bias for the 972-keV conversion electrons from ^{207}Bi was in the range of 15 to 23 keV (FWHM).

(B. H. Audet and D. M. Skopik)

The evaluation of silicon avalanche-type detectors for counting low-energy electrons and protons continued with an investigation of the temperature dependence of the leakage current, noise, and avalanche voltage of two typical units. At the operating bias (a few volts below the avalanche bias of about 200 V) the current remained constant when the detector temperature was between 23 and 30°C. Above 30°C, the current increased gradually; at 50°C its value was four times the value at 30°C. The noise increased only slightly over this temperature range. This may indicate that the principal source of noise in the avalanche detectors is not due to fluctuations in the thermally-generated carriers in the normal sense. Noise analysis in avalanche-type devices has been considered by Haitz and Smits [1] who showed that two noise sources in avalanche detectors can be related to the multiplication process.

The temperature coefficient of the avalanche bias for these two detectors was observed to be 0.1 percent/deg C for an operating temperature between 23 and 50°C. This variation of bias is acceptable for operation of these detectors in a spacecraft.

Radiation Damage — The effect of damage of 15-keV and 22-KeV protons on the current, capacitance, noise, and alpha-particle resolution of 100 μm thick, totally-depleted, surface-barrier detectors (Au-*n*-Si-Al) operating at room temperature was studied. Four different detectors with similar initial electrical and geometrical characteristics were irradiated, one detector for each combination of front- or rear-contact irradiation with 15- or 22-keV protons. Irradiation of the front (Au) contact at each energy produced damage effects similar to those observed in previous studies which used higher energy protons (50- to 800-keV). The current and noise increased with fluence, with a sharp increase in noise occurring at fluences of about 5×10^{13} protons/cm^2. The detector

capacitance increased with fluence for a reverse bias of less than a few volta, but was essentially unchanged with increasing fluence at the normal operating bias of 50 V. The degradation of energy resolution for monoenergetic alpha particles, incident on the front or rear contacts, was primarily due to the noise induced by damage to the front contact.

Irradiation of the rear (Al) contact at each energy produced only minor changes in the detector current, noise, capacitance, or energy resolution of alpha particles incident on the front (Au) contact, even for fluences of 1×10^{16} protons/cm^2. However, in this case, the detector energy resolution for alpha particles incident on the rear contact degraded with fluence and the spectral peak position decreased slightly whereas the noise remained essentially unchanged. This suggests that a dead layer was formed as a result of the proton damage at the rear contact, thus causing degraded energy resolution due to the poor collection of charge produced by alpha particles in that "dead" region. The presence of a relatively large electric field associated with the surface barrier at the front contact and the lower magnitude of fluence (by a factor of 500) may be the reasons why the dead layer effect was not observed for the front-contact irradiations. (J. A. Coleman and Y. M. Liu)

Plans: Detectors for use in space vehicles will be tested and evaluated. Evaluation of avalanche-type detectors for use in satellites and sounding rockets will continue with emphasis on the criterion of high detection efficiency for low-energy protons and electrons. Low-energy electron (<600 keV) damage effects in surface-barrier detectors will be studied if the accelerator is available.

4.5 REFERENCES

4.1 Thermal Properties of Devices

1. M. R. P. Young and D. A. Peterman, "Reliability Engineering," *Microelectronics and Reliability* 7, 91-103 (1968).

4.4 Silicon Nuclear Radiation Detectors

1. R. H. Haitz and F. M. Smits, "Nose Analysis for a Silicon Particle Detector with Internal Multiplication," *IEEE Trans. Nucl. Sci.* NS-13, No. 3, 198-207 (1966).

2. J. A. Coleman, D. P. Love, J. H. Trainor and D. J. Williams, "Low-Energy Proton Damage Effects in Silicon Surface-Barrier Detectors," *IEEE Trans. Nucl. Sci.* NS-15, No. 1, 482-490 (1968); "Effects of Damage by 0.8 MeV — 5.0 MeV Protons in Silicon Surface-Barrier Detectors," *IEEE Trans. Nucl. Sci.* NS-15, No. 3, 363-372 (1968).

Appendix A

JOINT PROGRAM STAFF

Coordinator: J. C. French
Consultant: C. P. Marsden

Semiconductor Characterization Section

Dr. W. M. Bullis, Chief

A. J. Baroody, Jr.
D. L. Blackburn
F. H. Brewer
Mrs. E. C. Cohen*
M. Cosman
Dr. J. R. Ehrstein
G. G. Harman
Mrs. R. E. Joel+
F. R. Kelly*
H. K. Kessler
Mrs. K. O. Leedy
Mrs. J. K. Madello*
R. L. Mattis
Dr. W. E. Phillips
Miss T. A. Poole+
Miss D. R. Ricks
H. A. Schafft
A. W. Stallings
G. N. Stenbakken
W. R. Thurber

Semiconductor Processing Section

Dr. J. A. Coleman, Chief

B. H. Audet
H. A. Briscoe
W. K. Croll
Mrs. S. A. Davis+
H. E. Dyson*
H. A. Gitelson*
W. J. Keery
E. I. Klein
J. Krawczyk
T. F. Leedy
Y. M. Liu
Miss J. M. Morrison
J. Oroshnik
D. M. Skopik
Dr. A. H. Sher
L. M. Smith
G. P. Spurlock

Electron Devices Section

J. C. French, Chief

Mrs. C. F. Bolton+
Mrs. R. Y. Cowan
Miss B. S. Hope+
R. L. Gladhill
J. M. Kenney
F. F. Oettinger
M. K. Phillips
R. C. Powell*
G. J. Rogers
S. Rubin
M. Sigman
L. Williams

---

* Part Time
\+ Secretary

APPENDIX B

STANDARDS COMMITTEE ACTIVITIES

ASTM Committee F-1; Materials for Electron Devices and Microelectronics
- F. H. Brewer, Resistivity Section
- W. M. Bullis, Editor, Subcommittee IV, Semiconductor Crystals
- J. A. Coleman, Secretary, Subcommittee V, Semiconductor Processing Materials
- J. R. Ehrstein, Epitaxial Resistivity and Epitaxial Thickness Sections
- J. C. French, Chairman, Subcommittee VIII, Editorial
- T. F. Leedy, Photomasking Section
- J. Oroshnik, Thin Films, Thick Films, and Photomasking Sections
- W. E. Phillips, Crystal Perfection, Encapsulation, Thin Films, and Thick Films Sections; Chairman, Lifetime Section
- A. H. Sher, Germanium Section
- M. Sigman, Editor, Subcommittee V, Semiconductor Processing Materials
- W. R. Thurber, Germanium and Impurities in Semiconductors Sections

Electronic Industries Association:
- F. F. Oettinger, Associate Member, MED 32, Active Digital Circuits; TG 41.6, Thermal Considerations, MED 41, Physical Characterization Requirements

Joint Electron Device Engineering Councils (EIA-NEMA):
- J. M. Kenney, Microwave Diode Measurements, JS-3, UHF and Microwave Diodes
- F. F. Oettinger, Technical Advisor on Thermal Resistance Measurements, JS-9, Low Power Transistors; Technical Advisor, JS-14, Thyristors
- R. C. Powell, Microwave Diode Measurement, JS-3, UHF and Microwave Diodes; Task Group on Transistor Scattering Parameter Measurement Standards, JS-9, Low Power Transistors.
- H. A. Schafft, Consultant on Second Breakdown Specifications, JS-6, Power Transistors

IEEE Electron Devices Group:
- J. M. Kenney, Chairman, Standards Committee Task Group on Microwave Solid State Devices II (Mixer and Video Detector Diodes)

IEEE Nuclear Science Group:
- J. A. Coleman, Administrative Committee; Nuclear Instruments and Detectors Committee; Editorial Board, *Transactions on Nuclear Science;* Chairman, 1970 Nuclear Science Symposium

IEEE Magnetics Group:
- S. Rubin, Chairman, Galvanomagnetic Standards Subcommittee

IEC TC47, Semiconductor Devices and Integrated Circuits:
- F. F. Oettinger, U. S. Experts Advisory Committee
- S. Rubin, Technical Expert, Galvanomagnetic Devices

NAS-NRC Ad Hoc Panel on Radiation Detectors and Associated Circuitry:
- J. A. Coleman

Appendix C

SOLID-STATE TECHNOLOGY AND FABRICATION SERVICES

Technical services in areas of competence are provided to other NBS activities and other government agencies as they are requested. Usually these are short-term, specialized services that cannot be obtained through normal commercial channels. Such services provided during the last quarter are listed below and indicate the kinds of technology available to the program.

1. Quartz and glass fabrication — (E. I. Klein)
   a. Five He-Ne gas laser tubes were rebuilt and one new tube was constructed for the Laboratory Astrophysics Division
   b. A 50-μm inside diameter, thick-walled capillary discharge tube was fabricated for the Radiation Thermometry Section.
   c. Two methane adsorption cells for use with lasers were made from quartz for the Engineering Metrology Section. The quartz end-windows for these cells had to be aligned and attached as precisely as those for a gas laser tube.
   d. Various jobs which required special fabrication and repair were carried out for the Instrument Shops Division and the Engineering Metrology Section.

2. Thin films — (W. K. Croll)
   A special pattern of aluminum metallization was deposited by vacuum evaporation on plastic sheet for the Instrumentation Applications Section.

3. Radiation detectors — (B. H. Audet and A. H. Sher)
   Assistance with reprocessing, testing and mounting semiconductor nuclear radiation detectors was provided for the Nuclear Spectroscopy Section and Photonuclear Physics Section.

4. Semiconductor crystal fabrication — (M. Cosman)
   a. A silicon internal reflection element was made for the Vacuum Measurements Section
   b. A silicon crystal was cut for the Mass and Volume Section

Appendix D

JOINT PROGRAM PUBLICATIONS

Prior Reports:

"Methods of Measurement for Semiconductor Materials, Process Control, and Devices, Quarterly Report, July 1 to September 30, 1968," NBS Tech. Note 472, December, 1968. (AD 681330)

"Methods of Measurement for Semiconductor Materials, Process Control, and Devices, Quarterly Report, October 1 to December 31, 1968," NBS Tech. Note 475, February, 1969. (AD 683808)

"Methods of Measurement for Semiconductor Materials, Process Control, and Devices, Quarterly Report, January 1 to March 31, 1969," NBS Tech. Note 488, July, 1969. (AD 692232)

"Methods of Measurement for Semiconductor Materials, Process Control, and Devices, Quarterly Report, April 1 to June 30, 1969." NBS Tech. Note 495, September, 1969. (AD 695820)

"Methods of Measurement for Semiconductor Materials, Process Control, and Devices, Quarterly Report, July 1 to September 30, 1969." NBS Tech. Note 520, March, 1970.

Current Publications

A. H. Sher and W. J. Keery, "Variation of the Effective Fano Factor in a Ge(Li) Detector," to appear in *IEEE Trans. Nucl. Sci.*, February, 1970.

J. L. Scales and W. M. Bullis, "Investigation of the Residual Defect in Indium Antimonide," to be presented at American Physical Society Meeting, Dallas, March, 1970, *Bull. APS* II, 15, 280 (1970).

A. H. Sher and J. A. Coleman, "Lithium Driftability in Detector Grade Germanium," accepted for presentation at 12th Scintillation and Semiconductor Counter Symposium, Washington, March, 1970; to appear in *IEEE Trans. Nucl. Sci.*, June, 1970.

J. A. Coleman, "Material Limitations on the Performance of Semiconductor Nuclear Radiation Detectors," accepted for presentation at 12th Scintillation and Semiconductor Counter Symposium, Washington, March, 1970; to appear in *IEEE Trans. Nucl. Sci.*, June, 1970.

R. C. Powell, "Precision Coaxial Connectors," a chapter to be published in *Advances in Microwaves* (Academic Press).

C. P. Marsden and R. Y. Cowan, "Tabulation of Data on Semiconductor Amplifiers and Oscillators at Microwave Frequencies," NBS Tech. Note 518, February, 1970.

NBS TECHNICAL PUBLICATIONS

PERIODICALS

JOURNAL OF RESEARCH reports National Bureau of Standards research and development in physics, mathematics, chemistry, and engineering. Comprehensive scientific papers give complete details of the work, including laboratory data, experimental procedures, and theoretical and mathematical analyses. Illustrated with photographs, drawings, and charts.

Published in three sections, available separately:

• Physics and Chemistry

Papers of interest primarily to scientists working in these fields. This section covers a broad range of physical and chemical research, with major emphasis on standards of physical measurement, fundamental constants, and properties of matter. Issued six times a year. Annual subscription: Domestic, $9.50; foreign, $11.75*.

• Mathematical Sciences

Studies and compilations designed mainly for the mathematician and theoretical physicist. Topics in mathematical statistics, theory of experiment design, numerical analysis, theoretical physics and chemistry, logical design and programming of computers and computer systems. Short numerical tables. Issued quarterly. Annual subscription: Domestic, $5.00; foreign, $6.25*.

• Engineering and Instrumentation

Reporting results of interest chiefly to the engineer and the applied scientist. This section includes many of the new developments in instrumentation resulting from the Bureau's work in physical measurement, data processing, and development of test methods. It will also cover some of the work in acoustics, applied mechanics, building research, and cryogenic engineering. Issued quarterly. Annual subscription: Domestic, $5.00; foreign, $6.25*.

TECHNICAL NEWS BULLETIN

The best single source of information concerning the Bureau's research, developmental, cooperative and publication activities, this monthly publication is designed for the industry-oriented individual whose daily work involves intimate contact with science and technology—*for engineers, chemists, physicists, research managers, product-development managers, and company executives.* Annual subscription: Domestic, $3.00; foreign, $4.00*.

* Difference in price is due to extra cost of foreign mailing.

NONPERIODICALS

Applied Mathematics Series. Mathematical tables, manuals, and studies.

Building Science Series. Research results, test methods, and performance criteria of building materials, components, systems, and structures.

Handbooks. Recommended codes of engineering and industrial practice (including safety codes) developed in cooperation with interested industries, professional organizations, and regulatory bodies.

Special Publications. Proceedings of NBS conferences, bibliographies, annual reports, wall charts, pamphlets, etc.

Monographs. Major contributions to the technical literature on various subjects related to the Bureau's scientific and technical activities.

National Standard Reference Data Series. NSRDS provides quantitive data on the physical and chemical properties of materials, compiled from the world's literature and critically evaluated.

Product Standards. Provide requirements for sizes, types, quality and methods for testing various industrial products. These standards are developed cooperatively with interested Government and industry groups and provide the basis for common understanding of product characteristics for both buyers and sellers. Their use is voluntary.

Technical Notes. This series consists of communications and reports (covering both other agency and NBS-sponsored work) of limited or transitory interest.

Federal Information Processing Standards Publications. This series is the official publication within the Federal Government for information on standards adopted and promulgated under the Public Law 89–306, and Bureau of the Budget Circular A–86 entitled, Standardization of Data Elements and Codes in Data Systems.

CLEARINGHOUSE

The Clearinghouse for Federal Scientific and Technical Information, operated by NBS, supplies unclassified information related to Government-generated science and technology in defense, space, atomic energy, and other national programs. For further information on Clearinghouse services, write:

Clearinghouse
U.S. Department of Commerce
Springfield, Virginia 22151

Order NBS publications from:

Superintendent of Documents
Government Printing Office
Washington, D.C. 20402

U.S. DEPARTMENT OF COMMERCE
WASHINGTON, D.C. 20230

OFFICIAL BUSINESS

POSTAGE AND FEES PAID
U.S. DEPARTMENT OF COMMERCE